Atmos. Chem. Phys. Discuss., doi:10.5194/acp-2016-1136, 2017
Manuscript under review for journal Atmos. Chem. Phys.
Discussion started: 2 March 2017

Atmospheric Chemistry and Physics Discussions

Seasonal and diurnal variations of methane and carbon dioxide in the Kathmandu Valley in the foothills of the central Himalaya

Khadak Singh Mahata[1,2], Arnico Kumar Panday [3,4], Maheswar Rupakheti[1,5*], Ashish Singh[1], Manish Naja[6], Mark G. Lawrence[1,2]

[1] Institute for Advanced Sustainability Studies (IASS), Potsdam, Germany

[2] University of Potsdam, Potsdam, Germany

[3] International Centre for Integrated Mountain Development (ICIMOD), Lalitpur, Nepal

[4] University of Virginia, Virginia, USA

[5] Himalayan Sustainability Institute (HIMSI), Kathmandu, Nepal

[6] Aryabhatta Research Institute of Observational Sciences (ARIES), Nainital, India

*Correspondence to: M. Rupakheti (maheswar.rupakheti@iass-potsdam.de)

Abstract

The SusKat-ABC (Sustainable Amosphere for the Kathmandu Valley- Atmospheric Brown Clouds) international air pollution measurement campaign was carried out during December 2012-June 2013 in the Kathmandu Valley and surrounding regions in Nepal. The Kathmandu Valley is a bowl-shaped basin with a severe air pollution problem. This paper reports measurements of two major greenhouse gases (GHGs), methane (CH_4) and carbon dioxide (CO_2), that begun during the campaign and extended for a year at the SusKat-ABC's supersite in Bode, a semi-urban location in the Kathmandu Valley. Measurements were also made at a nearby rural site (Chanban), ~25 km (aerial distance) to the southwest of Bode, on the other side of a tall ridge. The ambient mixing ratios of methane (CH_4), carbon dioxide (CO_2), water vapor, and carbon monoxide (CO) were measured with a cavity ring down spectrometer (Picarro G2401, USA), along with meteorological parameters for a year (March 2013 - March 2014).

Atmos. Chem. Phys. Discuss., doi:10.5194/acp-2016-1136, 2017
Manuscript under review for journal Atmos. Chem. Phys.
Discussion started: 2 March 2017

Atmospheric Chemistry and Physics Discussions

Simultaneous measurements were also made at Chanban from 15 July to 3 October 2015. These measurements are the first of their kind in the central Himalayan foothills. At Bode, the annual average mixing ratios of CO_2 and CH_4 were 419.4(±23.9) ppm and 2.193(±0.224) ppm, respectively. These values are higher than the levels observed at background sites such as Mauna Loa, USA (CO_2: 396.8 ppm, CH_4: 1.831 ppm) and Waliguan, China (CO_2: 397.7 ppm, CH_4: 1.879 ppm) during the same period, and at other urban/semi-urban sites in the region such as Ahmedabad and Shadnagar (India) and Nanjing (China). They varied slightly across the seasons at Bode, with seasonal average CH_4 mixing ratios being 2.157(±0.230) ppm in the pre-monsoon season, 2.199(±0.241) ppm in the monsoon, 2.210(±0.200) ppm in the post-monsoon, and 2.214(± 0.209) ppm in the winter season. The average CO_2 mixing ratios were 426.2(±25.5) ppm in pre-monsoon, 413.5(±24.2) ppm in monsoon, 417.3(±23.1) ppm in post-monsoon, and 421.9(±20.3) ppm in winter season. The maximum seasonal mean mixing ratio of CH_4 in winter was only 0.057 ppm or 2.6% higher than the seasonal minimum during the pre-monsoon period, while CO_2 was 12.8 ppm or 3.1% higher during the pre-monsoon period (seasonal maximum) than during the monsoon (seasonal minimum). On the other hand, the CO mixing ratio at Bode was 191% higher during the winter than during the monsoon season. The enhancement in CO_2 mixing ratios during the pre-monsoon season is associated with additional CO_2 emissions from forest fire and agro-residue burning in northern South Asia in addition to local emissions in the Kathmandu Valley. Published CO/CO_2 ratios of different emission sources in Nepal and India were compared with the observed CO/CO_2 ratios in this study. This comparison indicated that the major sources in the Kathmandu Valley were residential cooking and vehicle exhaust in all seasons except winter. In winter, the brick kiln emissions were a major source. Simultaneous measurement in Bode and Chanban (15 July-3 Oct 2015) revealed that the mixing ratio of CO_2, CH_4 and CO mixing ratios were 3.8%, 12%, and 64% higher in Bode than Chanban. Kathmandu Valley, thus, has significant emissions from local sources, which can also be attributed to its bowl shaped geography that is conducive to pollution build-up. All three gas species in Bode showed strong diurnal patterns, whereas CH_4 and CO at Chanban did not show any noticeable diurnal variations.

Atmos. Chem. Phys. Discuss., doi:10.5194/acp-2016-1136, 2017
Manuscript under review for journal Atmos. Chem. Phys.
Discussion started: 2 March 2017

These measurements provide the first insights into diurnal and seasonal variation of key greenhouse gases and air pollutants and their local and regional sources, which are important information for the atmospheric research in the region.

1 Introduction

The average atmospheric mixing ratios of two major greenhouse gases (GHGs), CO_2 and CH_4, have increased by about 40% (from 278 to 390.5 ppm) and about 150% (from 722 to 1803 ppb) respectively since pre-industrial times (~1750 AD). This is mostly attributed to anthropogenic emissions (IPCC, 2013). The current global annual rate of increase of the atmospheric CO_2 mixing ratio is 1-3 ppm, with average annual mixing ratios now exceeding a value of 400 ppm at the background reference location in Mauna Loa (WMO, 2016). Between 1750 and 2011, 555(±85) PgC of anthropogenic CO_2 was added to the atmosphere, of which two thirds were contributed by fossil fuel combustion and cement production, with the remaining coming from deforestation and land use/land cover changes (IPCC, 2013). CH_4 is the second largest gaseous contributor to anthropogenic radiative forcing after CO_2 (Forster et al., 2007). The major anthropogenic sources of atmospheric CH_4 are rice paddies, ruminants and fossil fuel use, contributing approximately 60% to the global CH_4 budget (Chen and Prinn, 2006; Schneising et al., 2009). The remaining fraction is contributed by biogenic sources such as wetlands and fermentation of organic matter by microbes in anaerobic conditions (Conrad, 1996).

Increasing atmospheric mixing ratios of CO_2 and CH_4 and other GHGs and short-lived climate-forcing pollutants (SLCPs) such as black carbon (BC) and tropospheric ozone (O_3) have caused the global mean surface temperature to increase by 0.85°C from 1880 to 2012. The surface temperature is expected to increase further by up to 2 degrees at the end of the 21st century in most representative concentration pathways (RCP) emission scenarios (IPCC, 2013). The increase in surface temperature is linked to melting of glaciers and ice sheets, sea level rise, extreme weather events, loss of biodiversity, reduced crop productivity, and economic losses (Fowler and Hennessy, 1995; Guoxin and Shibasaki, 2003).

Seventy percent of global anthropogenic CO_2 is emitted in urban areas (Fragkias et al., 2013). Developing countries may have lower per capita GHG emissions than developed countries, but

the large cities in developing countries, with their high population and industrial densities, are major consumers of fossil fuels and thus, emitters of GHGs. South Asia, a highly populated region with rapid growth in urbanization, motorization, and industrialization in recent decades, has an ever increasing fossil fuel demand and its combustion emitted 444 Tg C/year in 2000 (Patra, et al., 2013), or about 5% of the global total CO_2 emissions. Furthermore, a major segment of the population in South Asia has an agrarian economy and uses biofuel for cooking activities, which is an important major source of air pollutants and greenhouse gases in the region.

The emission and uptake of CO_2 and CH_4 follow a distinct cycle in South Asia. Ecosystem and inversion models show that the highest CO_2 release to the atmosphere occurs around April and May while the highest uptake occurs between July-October (Prasad et al., 2014). Patra et al. (2011) also showed that uptake peaks in August, using an inversion constrained by regional measurements from commercial aircraft. The observed trend is linked with the growing seasons. Agriculture is a major contributor of methane emission. For instance, in India it contributes to 75% of CH_4 emissions (MoEF, 2007). Ambient CH_4 concentrations are highest during June to September (peaking in September) in South Asia which are also the growing months for rice paddies (Goroshi et al., 2011). The minimum ambient CH_4 concentrations are observed in February-March (Prasad et al., 2014).

Climate change has impacted South Asia in several ways, as evident in temperature increase, change in precipitation patterns, higher incidence of extreme weather events (floods, droughts, heat waves, cold waves), melting of snowfields and glaciers in the mountain regions, and impacts on ecosystems and livelihoods (ICIMOD, 2009; MoE, 2011). Countries such as Nepal are vulnerable to impacts of climate change due to inadequate preparedness for adaptation to impacts of climate change (MoE, 2011). Decarbonization of its economy can be an important policy measure in mitigating climate change. Kathmandu Valley is one of the largest metropolitan cities in the foothills of the Hindu Kush-Himalaya which has significant reliance on fossil fuels and biofuels. In 2005, fossil fuel burning accounted for 53 % of total energy consumption in the Kathmandu Valley, while biomass and hydroelectricity were 38% and 9%, respectively (Shrestha and Rajbhandari, 2010). Fossil fuel consumed in the Kathmandu Valley

accounts for 32% of the country's fossil fuel imports, and the major fossil fuel consumers are residential (53.17%), transport (20.80%), industrial (16.84%), and commercial (9.11%) sectors. Combustion of these fuels in traditional technologies such as Fixed Chimney Bulls Trench Kiln (FCBTK) and low efficiency engines (vehicles, captive power generator sets etc.) emit significant amounts of greenhouse gases and air pollutants. This has contributed to elevated ambient concentrations of particulate matter (PM), including black carbon and organic carbon, and several gaseous species such as ozone, polycyclic aromatic hydrocarbons (PAHs), acetonitrile, benzene and isocyanic acid (Pudasainee et al., 2006; Aryal et al., 2009; Panday and Prinn, 2009; Sharma et al., 2012; World Bank, 2014; Chen et al., 2015; Putero et al., 2015: Sarkar et al., 2016). The ambient levels often exceed national air quality guidelines (Pudasainee et al., 2006; Aryal et al., 2009; Putero et al., 2015) and are comparable or higher than ambient levels observed in other major cities in South Asia.

Past studies in the Kathmandu Valley have focused mainly on a few aerosols species (BC, PM) and short-lived gaseous pollutants such as ozone and carbon monoxide (Pudasainee et al., 2006; Aryal et al., 2009; Panday and Prinn, 2009; Sharma et al., 2012, Putero et al., 2015). To the best of authors' knowledge, no direct measurements of CO_2 and CH_4 are available for the Kathmandu Valley. Recently, emission estimates of CO_2 and CH_4 were derived for the Kathmandu Valley using the International Vehicle Emission (IVE) model (Shrestha et al., 2013). The study estimated 1554 Gg of annual emission of CO_2 from a fleet of vehicles (that consisted of public buses, 3-wheelers, taxis and motor cycles; private cars, trucks and non-road vehicles were not included in the study) for the year 2010. In addition, the study also estimated 1.261 Gg of CH_4 emitted from 3 wheelers (10.6 %), taxis (17.7 %) and motorcycles (71 %) for 2010.

This study presents the first 12 months of measurements of two key GHGs, CH_4 and CO_2 along with other trace gases and meteorological parameters in Bode, a semi-urban site in the eastern part of the Kathmandu Valley. The year-long measurement in Bode is a part of the SusKat-ABC (Sustainable Atmosphere for the Kathmandu Valley – Atmospheric Brown Clouds) international air pollution measurement campaign conducted in and around the Kathmandu Valley from December 2012 to June 2013. Details of the SusKat-ABC campaign are described in Rupakheti et al. (2016, manuscript in preparation). The present study provides a detailed account of

seasonal and diurnal behaviors of CO_2 and CH_4 and their possible sources. To examine the rural-urban differences and estimate the urban enhancement, these gaseous species were also simultaneously measured for about three months (Jul-Oct) in 2015 at Chanban, a rural site about 25 km (aerial distance) outside and southwest of Kathmandu Valley. The seasonality of the trace gases and influence of potential sources in various (wind) directions are further explored by via ratio analysis. This measurement provides unique data from highly polluted but relatively poorly studied region (central Himalayan foothills in South Asia) which could be useful for validation of emissions estimates, model outputs and satellite observations. The study, which provides new insights on potential sources, can also be a good basis for designing mitigation measures for reducing emissions of air pollutants and controlling greenhouse gases in the Kathmandu Valley and the region.

2 Experiment and Methodology

2.1 Kathmandu Valley

The Kathmandu Valley consists of three administrative districts: Kathmandu, Lalitpur, and Bhaktapur, situated between 27.625° N, 27.75° N and 85.25°E, 85.375°E. It is a nearly circular bowl-shaped valley with a valley floor area of approximately 340 km^2 located at an altitude of 1300 m mean sea level (masl). The surrounding mountains are close to 2000-2800 in height above sea level with five mountain passes located at about 200-600 m above the valley floor and an outlet for the Bagmati River southwest of the Kathmandu Valley. Lack of decentralization in in Nepal has resulted in the concentration of economic activities, health and education facilities, the service sector, as well as most of the central governmental offices in the Kathmandu Valley. Consequently, it is one of the fastest growing metropolitan areas in South Asia with a current population of about 2.5 million, and the population growth rate of 4% per year (World Bank, 2013) Likewise, approximately 50% of the total vehicle fleet (2.33 million) of the country is in Kathmandu Valley (DoTM, 2015). The consumption of fossil fuels such as liquefied petroleum gas (LPG), kerosene for cooking and heating dominates the residential consumption, while the rest use biofuel (fuelwood, agro-residue, animal dung) for cooking and heating in the Kathmandu Valley. The commercial sector is also growing in the valley, and the latest data indicate the

Atmos. Chem. Phys. Discuss., doi:10.5194/acp-2016-1136, 2017
Manuscript under review for journal Atmos. Chem. Phys.
Discussion started: 2 March 2017

presence of 633 industries of various sizes. These are mainly associated with dyeing, brick kilns, and manufacturing industries. Fossil fuels such as coal and biofuels are the major fuels used in brick kilns. Brick kilns are reported as one of the major contributors of air pollution in the Kathmandu Valley (Chen et al., 2015; Kim et al., 2015; Sarkar et al., 2016). There are about 115 brick industries in the valley (personal communication with M. Chitrakar, President of the Federation of Nepalese Brick Industries). Acute power shortage in the Valley is common all around the year, especially in the dry season (winter/pre-monsoon) when the power cuts can last up to 12 hours a day (NEA, 2014). Energy demand during the power cut period is met with the use of small (67% of 776 generators surveyed for the World Bank study was with capacity less than 50kVA) but numerous captive power generators (diesel/petrol), which further contribute to valley's poor air quality. According to the World Bank's estimate, over 250,000 such generator sets are used in the Kathmandu Valley alone, producing nearly 200 MW of captive power, and providing about 28% of the total electricity consumption of the valley (World Bank, 2014). Apart from these sources, trash burning, which is a common practice (more prevalent in winter) throughout the valley, is one of the major sources of air pollutants and GHGs.

Climatologically, Kathmandu Valley has a sub-tropical climate with annual mean temperature of 18°C, and annual average rainfall of 1400 mm, of which 90% occurs in monsoon season (June-September). The rest of the year is dry with some sporadic rain events. The wind circulation at large scale in the region is governed by the Asian monsoon circulation and hence the seasons are also classified based on such large scale circulations and precipitation: Pre-Monsoon (March-May), Monsoon (June-September), Post-Monsoon (October-November) and Winter (December-February). Sharma et al. (2012) used the same classification of seasons while explaining the seasonal variation of BC concentrations observed in the Kathmandu Valley. Locally in the valley, the mountain-valley wind circulations play an important role in influencing air quality. The wind speed at the valley floor is calm (≤ 1 m s^{-1}) in the morning and night, while a westerly wind develops after 11:00 AM in the morning till dusk, and switches to a mild easterly at night (Panday and Prinn, 2009; Regmi et al., 2003). This is highly conducive to building up of air pollution in the valley, which gets worse during the dry season.

2.2 Study sites

Two sites, a semi-urban site within the Kathmandu Valley and a rural site outside the Kathmandu Valley, were selected for this study. The details of the measurements carried out in these sites is described Table 1 and in section 2.2.1 and 2.2.2.

2.2.1 Bode (SusKat-ABC supersite)

The SusKat-ABC supersite was set up at Bode, a semi-urban location (Figure 1) of the Madhyapur Thimi municipality in the Bhaktapur district in the eastern side of the Kathmandu Valley. The site is located at 27.68^{0}N latitude, 85.38^{0}E longitude, and 1344 masl. The local area around the site has a number of scattered houses and agricultural fields. The agriculture fields are used for growing rice paddies in the monsoon season. It also receives outflow of polluted air from three major cities in the valley: Kathmandu Metropolitan City and Lalitpur Sub-metropolitan City, both mainly during daytime, and Bhaktapur Sub-metropolitan City mainly during nighttime. Among other local sources around the site, about 10 brick kilns are located in the east and southeast direction, approximately within 1-4 km from the site which are operational only during dry season (January to April). There are close to 20 small and medium industries (pharmaceuticals, plastics, electronics, tin, wood, aluminum, iron, and fabrics etc.) scattered in the same direction. The Tribhuvan International Airport (TIA) is located approximately 4 km away to the west of the Bode site.

2.2.2 Chanban

Chanban is a rural/background site in Makwanpur district outside of the Kathmandu Valley (Figure 1). This site is located ~25 km aerial distance due southwest from Bode. The site is located on a small ridge (27.65^{0}N, 85.14^{0}E, 1896 masl) between two villages - Chitlang and Bajrabarahi - within the forested watershed area of Kulekhani Reservoir, which is located ~ 4.5 km southwest of the site. The instruments were set up on the roof of 1-storey building in an open space inside the Nepali Army barrack. There was a kitchen of the army barrack at about 100 m to the southeast of the measurement site. The kitchen uses LPG, electricity, kerosene, and firewood for cooking activities.

2.3 Instrumentation

The measurements were carried out in two phases in 2013-2014 and 2015. In phase one, a cavity ring down spectrometer (Picarro G2401, USA) was deployed in Bode to measure ambient CO_2, CH_4, CO, and water vapor mixing ratios. Twelve months (6 March 2013 - 5 March 2014) of continuous measurements were made in Bode. The operational details of the instruments deployed in Bode are also provided in Table 1. In phase two, simultaneous measurements were made in Bode and Chanban for a little less than 3 months (15 July to 03 October 2015).

The Picarro G2401 analyzer quantifies spectral features of gas phase molecules by using a novel wavelength-scanned cavity ring down spectroscopic technique (CRDS). The instrument has a 30 km path length in a compact cavity that results high precision and sensitivity. Because of the high precision wavelength monitor, it uses absolute spectral position and maintains accurate peak quantification. Further, it only monitors the special features of interest for reducing the drift. The instrument also has water correction to report dry gas fraction. The reported measurement precision for CO_2, CH_4, CO and water vapor in dry gas is < 150 ppb, < 30 ppb, < 1ppb and < 200 ppm for 5 seconds with 1 standard deviation (Picarro, 2015).

In Bode, the Picarro analyzer was placed on the 4th floor of a 5-storey building with an inlet at 0.5 m above the roof of the building with a 360 degree view (total inlet height: 20 m above ground). The sample air was filtered at the inlet to keep dust and insects out and was drawn into the instrument through a 9 m Teflon tube (1/4 inches ID). The Picarro analyzer was set to record data in every 5 second and recorded both directly sampled data and water corrected data of CO_2 and CH_4. In this paper, only water-corrected or dry mixing ratios of CH_4 and CO_2 were used to calculate the hourly averages for diurnal and seasonal analysis.

The instruments were factory calibrated before commencing the field measurement. Picarro G2401 model is designed for remote application and long term deployment with minimal drift and less requirement for intensive calibration (Crosson, 2008) and thus was chosen for the current study in places like Kathmandu where there is no or limited availability of high quality reference gases. Regular calibration of Picarro G2401 in field during 2013-2014 deployment was not conducted due to challenges associated with the quality of the reference gas, especially for CO and CH_4. One time calibration was performed for CO_2 (at 395, and 895 ppmv) in July 2015

before commencing the simultaneous measurement in Bode and Chanban in 2015. The % difference of the analyzer differed by approximately 5% at reference mixing ratio. CO observations from Picarro G2401 were compared with observations from another CO analyzer (Horiba, model AP370) that was also operated in Bode for 3 months (March - May 2013). Horiba CO monitor was a new unit, which was factory calibrated before its first deployment in Bode. Nevertheless, this instrument was inter-compared with another CO analyzer (same model) from the same manufacturer prior to the campaign and its correlation coefficient was 0.9 [slope of data from the new unit (y-axis) vs the old unit (x-axis) = 1.09]. Primary gas cylinders from Linde UK (1150 ppbv) and secondary gases from Ultra-Pure Gases and Chemotron Science Laboratories (1790 ppbv) were used for the calibration of CO instrument. Further details on CO measurements and calibration of Horiba AP370 can be found in Sarangi et al. (2014; 2016). Statistically significant correlation (r = 0.99, slope = 0.96) was found between Picarro and Horiba hourly average CO mixing ratio data (Supplementary Information Figure S1). Furthermore, the monthly mean difference between these two instruments (Horiba AP370 minus Picarro G2401) was calculated to be 0.02 ppm (3%), 0.04 ppm (5%) and 0.02 ppm (4%) in March, April and May, respectively. For the comparison period of 3 months, the mean difference was 0.02 ppm (4%). Overall differences were small to negligible during the comparison period and thus, adjustment in the data was deemed not necessary.

Besides highly selective to individual species, Picarro G2401 has a water correction function and thus accounts for the any likely drift in CO, CO_2 and CH_4 mixing ratios with the fluctuating water vapor concentration (Chen et al., 2013;Crosson, 2008). Crosson (2008) also estimated a peak to peak drift of 0.25 ppmv. Further, Crosson (2008) observed a 1.2 ppbv/day drift in CO_2 after 170 days from the initial calibration. For a duration of one year the drift will be less than 1 ppmv, which is less than 1% of the observed mixing ratio in (hourly ranges: 376-537 ppm) Bode even if the drift was in same magnitude as in case of Crosson (2008). Crosson (2008) reported 0.8 ppbv peak to peak drift in CH_4 measurements for 18 days after the initial calibration.

There were other instruments concurrently operated in Bode; a ceilometer for measuring mixing layer height (Vaisala Ceilometer CL31, Finland), and an Automatic Weather Station (AWS) (Campbell Scientific, USA). The ceilometer was installed on the rooftop (20 m above ground) of

the building (Mues et al., 2017). For measuring the meteorological parameters, a Campbell Scientific AWS (USA) was set up on the roof of the building with sensors mounted at 2.9 m above the surface of the roof (22.9 m from the ground). The Campbell Scientific AWS measured wind speed and direction, temperature, relative humidity and solar radiation every minute. Temperature and rainfall data were taken from an AWS operated by the Department of Hydrology and Meteorology (DHM), Nepal at the Tribhuvan International Airport (TIA, see Figure 1), ~4 km due west of Bode site.

At Chanban, the inlet for Picarro gas analyzer was kept on the rooftop ~3 m above the ground and the sample air was drawn through a 3 m long Teflon tube (1/4 inches ID). The sample was filtered at the inlet with a filter (5-6 µm pore size) to prevent aerosol particles from getting into the analyzer. An automatic weather station (Davis Vantage Pro2, USA) was also set up in an open area, about 17 m away from the building and with the sensors mounted at 2 m above ground.

3. Results and discussion

The results and discussions are organized as follow: Sub-section 3.1 describes a year round variation in CH_4, CO_2, CO and water vapor at Bode; sub-sections 3.2, 3.3 and 3.4 present the analysis of the observed diurnal, monthly, seasonal variations. Sub-sections 3.5, 3.6, 3.7 discusses the impact of city pollution at the measurement site at Bode, influence of regional pollution and potential sources in the valley and sub-section 3.8 compares and contrasts CH_4, CO_2, CO at Bode and Chanban.

3.1 Time series of CH_4, CO_2, CO and water vapor mixing ratios

Figure 2 shows the time series of hourly mixing ratios of CH_4, CO_2, CO, and water vapor at Bode. Meteorological data from Bode and the Tribhuvan International Airport are also shown in Figure 2. Data gaps in Figure 2a and 2b were due to maintenance of the measurement station. In general, the changes observed in CO mixing ratio was higher in terms of % change than the variations observed in CH_4 and CO_2 mixing ratios during the sampling period. In contrast, CO mixing ratios decreased and water vapor mixing ratios increased significantly during the rainy

Atmos. Chem. Phys. Discuss., doi:10.5194/acp-2016-1136, 2017
Manuscript under review for journal Atmos. Chem. Phys.
Discussion started: 2 March 2017

Atmospheric Chemistry and Physics Discussions

season (June-September). For the entire sampling period, the annual average CH_4, CO_2, CO, and water vapor mixing ratios were 2.193 (± 0.224) ppm, 419.4 (± 23.9) ppm, 0.50 (± 0.35) ppm, and 1.71 (± 0.71) %, respectively. The annual CH_4 and CO_2 mixing ratios were compared to the historical background site (Mauna Loa Observatory, Hawaii, USA) and the background site (Waliguan, China) in Asia, which will provide insight on spatial differences. The selection of neighboring countries' (i.e., India and China's) urban and semi-urban sites, where many emission sources are typical for the region, for comparison provides information on relative differences (higher/lower), which will help in investigating possible local emission sources in the valley. As expected, annual mean of CH_4 and CO_2 mixing ratios in the Kathmandu Valley were higher than the levels observed at background sites in the region and elsewhere for the same period (Table 4). CH_4 was nearly 20% higher at Bode than at Mauna Loa observatory (1.831 ppm) (Dlugokencky et al., 2016) and 17% higher than at Mt. Waliguan (1.879 ppm) in China for the same observation period (Dlugokencky et al., 2016). The small difference between Bode and Waliguan in comparison to Mauna Loa Observatory indicates the higher mixing ratio of CH_4 in Asia region. It could be associated with agricultural activities in this region. Similarly, the annual CH_4 at Bode was higher than urban/semi-urban sites in India, such as an urban site in Ahmedabad (1.880 ppm) (Sahu and Lal, 2006) and Shadnagar (1.92 ± 0.07), a semi-urban site in Telangana state (~70 km north from Hyderabad city) during 2014 (Sreenivas et al., 2016). Likewise, the annual average CO_2 mixing ratio at Bode (419.4 ppm) during the observation period was 5.7% higher than at Mauna Loa Observatory (396.76 ppm) (Tans and Keeling, 2014) and 5.5% higher than at Mt. Waliguan (397.7 ppm). The CO_2 mixing ratio in the Kathmandu Valley was also found to be higher than the levels observed in Shadnagar (394 ± 2.9 ppm) during 2014, Ahmedabad city (413 ± 13.7 ppm) in India during November 2013 to May 2015, and an urban site at Nanjing (406.5 ± 20 ppm) in China (Huang et. al., 2015; Sreenivas et al., 2016; Chandra et al., 2016).

The high CH_4 and CO_2 mixing ratios at Bode in comparison to Ahmedabad, Shadnagar and Nanjing could be due to more than 115 coal-biomass fired brick kiln, some of them are located near the site (less than 4 km) and confinement of pollutants within the Valley due to bowl shaped topography of the Kathmandu Valley. Although Ahmedabad and Nanjing sites are in big cities

with high population larger than Kathmandu Valley but they are far from the nearby heavy polluting industries and situated in plains, where ventilation of pollutants would be more efficient as opposed to the Kathmandu Valley. The major polluting sources were industries, residential cooking and transport sector in Ahmedabad (Chandra et al., 2016). Anthropogenic emission, synoptic circulation, terrestrial biosphere had important role on CO_2 mixing ratios in Nanjing (Huang et al., 2015). Shadnagar is a small town with a population of 0.16 million and major sources were industries (small-medium), biomass burning in residential cooking (Sreenivas et al., 2016).

The monthly average of CO_2 mixing ratios in 2015 in Chanban (Aug: 403.4, Sep: 399.1 ppm) were slightly higher than the background sites at Mauna Loa Observatory (Aug: 398.89 ppm, Sep: 397.63 ppm) and Mt. Waliguan (Aug: 394.55 ppm, Sep: 397.68 ppm) (Dlugokencky et al., 2016). For these two months in 2015, CH_4 mixing ratios were also higher in Bode (Aug: 2281.11 ppb, Sep: 2370.93 ppb) and Chanban (Aug: 2049.71 ppb, Sep: 2101.75 ppb) compared to Mauna Loa Observatory (Aug: 1831.04 ppb, Sep: 1845.68 ppb) (Dlugokencky et al., 2016)) and Mt. Waliguan (Aug: 1914.99 ppb, 1911.21 ppb) (Dlugokencky et al., 2016). The low differences in CO_2 between Chanban and background sites mentioned above indicate the less number of and/or less intense CO_2 sources at Chanban during these months because of the lack of burning activities due to rainfall in the region. However, high CH_4 values in August and September in Bode, Chanban and Mt. Waliguan in comparison to Mauna Loa Observatory may indicate the influence of CH_4 emission from paddy fields in the Asian region.

3.2 Monthly and Seasonal variations

Figure 3 shows the monthly box plot of hourly CH_4, CO_2, CO and water vapor observed for a year in Bode. Monthly and seasonal averages of CH_4 and CO_2 mixing ratios at Bode are summarized in Table 2 and 3. CH_4 were lowest during May-July (ranges from 2.093-2.129 ppm) period and highest during August-September (2.274-2.301 ppm), followed by winter. In addition to the influence of active local sources, the shallow boundary layer in winter was linked to elevated concentrations (Panday and Prinn, 2009; Putero et al., 2015, Mues et al., 2016). The low CH_4 values from May to July may be associated with the absence of brick kiln and frequent

366 rainfall in these months. Brick kiln were operational during January to April. Rainfall also leads
367 to suppression of open burning activities in the valley (see Figure 2b). The CH_4 was slightly
368 higher (statistically significant, $p<0.05$) in monsoon season (July –September) than pre-monsoon
369 season (unlike CO_2 which was higher in pre-monsoon), and could be associated with the addition
370 of CH_4 flux from the water-logged rice paddies (Goroshi et al. (2011). There was a visible drop
371 in CH_4 from September to October but remained consistently over 2.183 ppm from October to
372 April with little variation between these months. Rice-growing activities are minimal or none in
373 October and beyond, and thus may be related to the observed dip in CH_4 mixing ratio.

374 Comparison of seasonal average CH_4 mixing ratios at Bode and Shadnagar (a semi-urban site in
375 India) indicated that CH_4 mixing ratios at Bode were higher in all seasons than at Shadnagar:
376 pre-monsoon (1.89 ± 0.05 ppm), monsoon (1.85 ± 0.03 ppm), post-monsoon (2.02 ± 0.01 ppm),
377 and winter (1.93 ± 0.05 ppm) (Sreenivas et al., 2016). The possible reason for lower CH_4 at
378 Shadnagar in all season could be associated with geographical location and difference in local
379 emission sources. The highest CH_4 mixing ratio in Shadnagar was reported in post-monsoon
380 which was associated with harvesting in the Kharif season (July – October), while the minimum
381 was in monsoon. Shadnagar is a relatively small city (population: ~0.16 million) compared to
382 Kathmandu Valley and the major local sources which may have influence on CH_4 emission
383 include bio-fuel, agro-residue burning and residential cooking.

384 The seasonal variation in CO_2 generally reflects the seasonality of major emission sources such
385 as brick kilns and regional emission sources such as vegetation fire and agriculture residue burn.
386 The concentrations of most pollutants in the region are lower during the monsoon period
387 (Sharma et al., 2012, Marinoni, 2013; Putero et al., 2015) due to limited emission sources and
388 partially due to rain washout. Monsoon is also the growing season with higher CO_2 assimilation
389 by plants than other seasons (Sreenivas et al., 2016). In contrast, winter, pre-monsoon and post-
390 monsoon season experiences an increase in emission activities in the Kathmandu Valley (Putero
391 et al., 2015).

392 The CO_2 mixing ratios were in the range of 376 - 537 ppm for the entire observation period.
393 Differences with CH_4 were observed in September and October where CO_2 was increasing

394 (mean/median) in contrast to CH_4 which showed the opposite trend. The observed increase in
395 CO_2 after October may be related to less or no rainfall, which results in the absence of rain-
396 washout and/or no suppression of active emission sources such as open burning activities. CO_2
397 remains relatively lower during July-August, but it is over 420 ppm from January to May.
398 Seasonal variation of CO_2 in Bode was similar in seasonal variation but the values are higher
399 than the values observed in Shadnagar, India (Sreenivas et al., 2016).

400 The variations in CO were more distinct than CH_4 and CO_2 during the observation period
401 (Figure 3). The highest CO values were observed from January-April (0.71-0.91 ppm). The
402 seasonal mean of CO mixing ratios at Bode were: pre-monsoon (0.60 ±0.36 ppm), monsoon
403 (0.26±0.09 ppm), post-monsoon (0.40±0.15 ppm), and winter (0.76±0.43 ppm). The maximum
404 CO was observed in winter, unlike CO_2 which was maximum in pre-monsoon. The high CO in
405 winter was due to the presence of strong local pollution sources (Putero et al., 2015) and shallow
406 mixing layer heights. The addition of regional forest-fire and agro-residue burning augmented
407 CO_2 mixing ratios in pre-monsoon. The water vapor mixing ratio showed a seasonal pattern
408 opposite of CO, with a maximum in monsoon (2.53 %) and minimum in winter (0.95 %), and
409 intermediate values of 1.56 % in pre-monsoon and 1.55 % in post-monsoon season.

410 There were days in August-September when the CH_4 increases by more than 3 ppm (Figure 2).
411 Enhancement in CO_2 was also observed during the same time period. It is likely that these high
412 enhancements were associated with the air mass from Northeast-East (NE-E) which had > 2.5
413 ppm CH_4 and > 450 CO_2 (see Figure 4). CO during the same period was not enhanced and didn't
414 show any particular directionality compared to CH_4 and CO_2 (not shown in Figure 4). Areas NE-
415 E to Bode are predominantly irrigated (rice paddies) during August-September, and sources such
416 as brick kilns were not operational during this time period. Goroshi et al. (2011) reported that
417 June to September is a growing season for rice paddies in South Asia with high CH_4 emissions
418 during these months and observed a peak in September in the atmospheric CH_4 column over
419 India. Model analysis also points to high methane emissions in September which coincides with
420 the growing period of rice paddies (Goroshi et al., 2011, Prasad et al., 2014). The CH_4 mixing
421 ratios at Bode in January (2.233 ± 0.219 ppm) and July (2.129 ± 0.168 ppm) were slightly higher
422 than the observation in Darjeeling (Jan: 1.929±0.056 ppm; Jul: 1.924±0.065 ppm), a hill station

of eastern Himalaya (Ganesan et al., 2013). The higher CH_4 values in January and July at Bode compared to Darjeeling could be because of the influence of local sources, in addition to the shallow boundary layer in Kathmandu Valley. Trash burning and brick kilns are two major sources from December until April in the Kathmandu Valley while emission from paddy fields occurs during July-September in the Kathmandu Valley. In contrast, the measurement site in Darjeeling was located at higher altitude (2194 masl) and was less influenced by the local emission. The measurement in Darjeeling reflected a regional contribution. There are limited local source in Darjeeling such as wood biomass burning, natural gas related emission and vehicular emission (Ganesan et al., 2013).

The period between January and April had generally higher or the highest values of CO_2, CH_4 and CO at Bode. The measurement site was impacted mainly by local Westerly-Southwesterly winds (W-SW) and East-Southeast (E-SE). The W-SW typically has a wind speed in the range ~1 - 6 m s^{-1} and was active during late morning to afternoon period (~11:00 to 17:00 NST, supplementary information Figure S2 and S3). Major cities in the valley such as Kathmandu Metropolitan City and Lalitpur Sub-metropolitan City are W-SW of Bode (Figure 1c). Wind from E-SE were generally calm ($\leq$1m s^{-1}) and observed only during night and early morning hours (21:00 to 8:00 NST). The mixing ratio of all three species in air mass from the E-SE was significantly higher than in the air mass from W-SW (Figure 4). There are 10 biomass co-fired brick kilns and Bhaktapur Industrial Estate located within 1-4 km E-SE from Bode (Sarkar et al., 2016). The brick kilns were only operational during January-April. Moreover, there were over 100 brick kilns operational in the Kathmandu Valley (Putero et al., 2015) which use low-grade lignite coal imported from India and biomass fuel to fire bricks in inefficient kilns (Brun, 2013).

Fresh emissions from main city center were transported to Bode during daytime by W-SW winds which mainly include vehicular emission. Compared to monsoon months (June-August), air mass from W-SW had higher values in all three species (Figure 4) during winter and pre-monsoon months. This may imply that in addition to vehicular emission, there are other potential sources which were exclusively active during these dry months. Municipal trash burning is also common in the Kathmandu Valley, with a reported higher frequency from December to February (Putero et al., 2015). The frequency in the use of captive power generator sets are highest during

452 the same period, which is another potential source contributing to air coming from W-SW
453 direction (World Bank, 2014; Putero et al., 2015).

454 Regional transport of pollutants into the Kathmandu Valley was reported by Putero et al. (2015).
455 The westerly circulation (originated at longitude about 60^0E in 5 days back trajectories) was
456 dominant from March-May 2013. Other sources of CO_2 and CH_4 could be due to vegetation fires
457 which were also reported in the region surrounding the Kathmandu Valley during the pre-
458 monsoon months (Putero et al., 2015). Similarly, high pollution events, peaking in the pre-
459 monsoon, were observed at Nepal Climate Observatory-Pyramid (NCO-P) near Mt. Everest,
460 which have been associated with vegetation fires in the Himalayan foothills and northern IGP
461 region (Putero et al., 2014). MODIS derived forest counts (Figure 5), which also indicated high
462 frequency of forest fire and farm fire from February to April and also during post-monsoon
463 season. It is interesting that the monthly mean CO_2 mixing ratio was maximum in April (430 ±
464 27 ppm) which could be linked to the fire events. It is likely that the westerly winds (>2.5-4.5 m
465 s^{-1}) during the daytime (supplementary information Figure S2, S3) bring additional CO_2 from
466 vegetation fires and agro-residue burning in southern plains of Nepal including the IGP region
467 (Figure 5). Low values of CO_2 and CH_4 during June-July (Figure 3) was coincident with the
468 rainy season, and sources such as brick kiln emission, trash burning, captive power generators,
469 and regional agriculture residue burning and forest fires are weak or absent during these months.

470 **3.3 Diurnal Variation**

471 Figure 6 shows the average seasonal diurnal patterns of CH_4, CO_2, CO, and water vapor mixing
472 ratios observed at Bode for four seasons. All the three gas species had a distinct diurnal pattern in
473 all seasons, characterized by maximum values in the morning hours (peaked around 7:00-9:00),
474 afternoon minima around 15:00-16:00, and a gradual increase through the evening until next
475 morning. There was no clear evening peak in CH_4 and CO_2 mixing ratios whereas CO shows an
476 evening peak around 20:00. The well-defined morning and evening peaks observed in CO
477 mixing ratios are associated with the peaks in traffic and residential activities. The CH_4 and CO_2
478 showed pronounced peaks in the morning hours (7:00-9:00) in all seasons with almost the same
479 level of seasonal average mixing ratios. CO had a prominent morning peak in winter and pre-

480 monsoon season, but the peak was significantly lower in monsoon and post-monsoon. The CO
481 (~1-1.4 ppm) around 8:00-9:00 am in winter and pre-monsoon were nearly 3-4 times higher than
482 in monsoon and post-monsoon season. It appears that CH_4 and CO_2 mixing ratios were
483 continuously building up at night until the following morning peak in all seasons. The similar
484 seasonal variations in CH_4 and CO_2 across all seasons could be due to their long-lived nature, as
485 compared to CO, whose diurnal variations are strongly controlled by the evolution of the
486 boundary layer. Kumar et al. (2015) also reported morning and evening peaks and an afternoon
487 low in CO_2 mixing ratios in industrial, commercial, and residential sites in Chennai in India. The
488 authors also found high early morning CO_2 mixing ratios at all sites and attributed it to the
489 temperature inversion and stable atmospheric condition.

490 The daytime low CH_4 and CO_2 mixing ratios were due to (i) elevated mixing layer height in the
491 afternoon (Figure 7), (ii) development of upslope wind circulation in the valley, and (iii)
492 development of westerly and southwesterly winds which blows through the valley during the
493 daytime from around 11 am to 5 pm (supplementary information Figure S2), all of which aid in
494 dilution and ventilation of the pollutants out of the valley (Regmi et al., 2003; Kitada and Regmi,
495 2003; Panday and Prinn, 2009). In addition, the daytime CO_2 minimum in the summer monsoon
496 is also associated with high photosynthetic activities in the valley as well as in the broader
497 surrounding region. In the nighttime and early morning, the mixing layer height was low (only
498 around 200-300 m in all seasons) and stable boundary layer for almost 17 hours a day. In the
499 daytime it grows up to 800-1200 m for a short time (ca. from 11:00 to 6:00) (Mues et al., 2016,
500 manuscript submitted to ACPD). Therefore the emissions from various activities in the evening
501 after 18:00 (cooking and heating, vehicles, trash burning, and bricks factories in the night and
502 morning) were trapped within the collapsing and shallow boundary layer, and hence mixing
503 ratios were high during evening, night and morning hours. Furthermore, plant and soil respiration
504 also increases CO_2 mixing ratio during the night (Chandra et al., 2016). However, Ganesan et al.
505 (2013) found a distinct diurnal cycle of CH_4 mixing ratios with twin peaks in the morning (7:00-
506 9:00), and afternoon (15:00-17:00) and a nighttime low in winter but no significant diurnal cycle
507 in the summer of 2012 in Darjeeling, a hill station (2194 masl) in the eastern Himalaya. The
508 authors described that the morning peaks could be due to the radiative heating of the ground in

509 the morning, which breaks the inversion layer formed during night, and as a result, pollutants are
510 ventilated from the foothills up to the site. The late afternoon peaks match wind direction and
511 wind speed (upslope winds) that could bring pollution from plains to mountains.

512 The diurnal variation of CO is also presented along with CO_2 and CH_4 in Figure 6c. CO is an
513 indicator of primary air pollution. Although CO mixing ratio showed distinct diurnal pattern, it
514 was different from the diurnal patterns of CO_2 and CH_4. CO diurnal variation showed distinct
515 morning and evening peaks, afternoon minima, and a nighttime accumulation or decay.
516 Nighttime accumulation in CO was observed only in winter and pre-monsoon and decay or
517 decrease in monsoon season and post-monsoon season (Figure 7). The lifetime of CO (weeks to
518 months) is very long compared to the ventilation timescales for the valley, so the different
519 diurnal cycles would be due to differences in nighttime emissions. While the biosphere respires
520 at night, most CO sources except brick kilns remain shut down late at night. This also explains
521 why nighttime values of CO drop less in the winter and pre-monsoon than in other seasons.
522 Furthermore, the prominent morning peaks of CO in pre-monsoon and winter compared to other
523 seasons results from nighttime accumulation, additional fresh emissions in the morning and
524 recirculation of the pollutants due to downslope katabatic winds (Pandey and Prinn, 2009;
525 Panday et al., 2009). Pandey and Prinn (2009) observed nighttime accumulation and gradual
526 decay during the winter (January 2005). The measurement site in Pandey and Prinn (2009) was
527 near the urban core of the Kathmandu Valley and had significant influence from the vehicular
528 sources all over the season including the winter season. Measurement in Bode lies in close
529 proximity to the brick kilns which operate 24 hours during the winter and pre-monsoon period.
530 Calm southeasterly winds are observed during the nighttime and early morning (ca.22:00 – 8:00)
531 in pre-monsoon and winter, which transport emissions from brick kiln to the site (Sarkar et al.,
532 2016). Thus the gradual decay in CO was not observed in Bode.

533 The timing of the CO morning peak observed in this study matches with observations by Panday
534 et al. (2009). They also found CO morning peak at 8:00 in October 2004 and at 9:00 in January
535 2005. The difference could be linked to the boundary layer stability. As the sun rises later in
536 winter, the boundary layer stays stable for a longer time in winter keeping mixing ratios higher in
537 morning hours than in other seasons with an earlier sunrise.

538 The morning peaks of CO_2 and CH_4 mixing ratios occurred around 6:00-7:00 local time in the
539 pre-monsoon, monsoon, and post monsoon season, whereas in winter their peaks are delayed by
540 1-2 hours in the morning; CH_4 at 8:00 and CO_2 at 9:00. The CO showed that its morning peak
541 was delayed compared to CO_2 and CH_4 morning peaks by 1-2 hour in pre-monsoon, monsoon
542 and post-monsoon (at 8:00) and in winter (at 9:00). The occurrence of morning peaks in CO_2 and
543 CH_4 1-2 hours earlier than CO is interesting. This could be due to the long lifetimes and
544 relatively smaller local sources of CH_4 and CO_2, as CO is mainly influenced by emissions from
545 vehicles during rush hour, as well as from biomass and trash burning in the morning hours. Also,
546 CO increases irrespective of change in mixing layer (collapsing or/rising, Figure 7) but CO_2 and
547 CH_4 start decreasing only after the mixing layer height starts to rise. Recently, Chandra et al.
548 (2016) also reported that the CO_2 morning peak occurred earlier than CO in observations in
549 Ahmedabad City India. This was attributed to CO_2 uptake by photosynthetic activities after
550 sunrise but CO kept increasing due to emissions from the rush hour activities.

551 Highest daytime minimum of CO_2 was observed in pre-monsoon which may indicate the
552 influence of regional emissions that increased the baseline background concentrations as well.
553 The daytime minimum mixing ratios occurs from 12:00 to 17:00 LST. The highest minimum
554 CO_2 was found in pre-monsoon (Figure 6b). Although the local emission sources are similar in
555 pre-monsoon and winter, the higher minimum daytime CO_2 mixing ratios in pre-monsoon season
556 than other seasons, suggest the influence of regional emissions in the Kathmandu Valley, which
557 has been reported in previous study by Putero et al. (2015). In monsoon and post-monsoon
558 seasons, the minimum CO_2 mixing ratios in the afternoon drops down to 390 ppm, which were
559 close to the value observed at the regional background sites such as Mauna Loa and Waliguan.

560 **3.4 Seasonal interrelation of CO_2, CH_4 and CO**

561 The Pearson's correlation coefficient (r) between CO_2 and CO was strong in winter (0.87),
562 followed by monsoon (0.64), pre-monsoon (0.52) and post-monsoon (0.32). The higher
563 coefficient in winter indicates that common or similar sources for CO_2 and CO and moderate
564 values in pre-monsoon and monsoon indicates the likelihood of different sources. To avoid the
565 influence of strong diurnal variations observed in the valley, daily averages, instead of hourly,

were used to calculate the correlation coefficients. The correlation coefficients between daily CH_4 and CO_2 for four seasons are as follows: winter (0.80), post-monsoon (0.74), pre-monsoon (0.70) and monsoon (0.22). A semi-urban measurement study in India also found a strong positive correlation between CO_2 and CH_4 in the pre-monsoon (0.80), monsoon (0.61), post-monsoon (0.72) and winter (0.8) (Sreenivas et al., 2016). It should be noted here that Sreenivas et al., (2006) used hourly average CO_2 and CH_4 mixing ratios. The weak monsoon correlation at Bode, which is in contrast to Sreenivas et al. (2016), may point to the influence of dominant CH_4 emission from paddy field during the monsoon season (Goroshi et al., 2011). Daily CH_4 and CO was also weakly correlated in monsoon (0.34) and post-monsoon (0.45). Similar to CH_4 and CO_2, the correlation between CH_4 and CO were moderate to strong in pre-monsoon (0.76) and winter (0.75).

Overall, the positive and high correlations between CH_4 and CO mixing ratios and between CH_4 and CO_2 in pre-monsoon and winter indicate common sources or source regions, most likely combustion related sources such as vehicular emission, brick kilns, agriculture fire etc. Weak correlation, between CH_4-CO_2 and between CH_4-CO, during monsoon season indicates sources other than combustion-related may be active, such as agriculture as a key CH_4 source (Goroshi et al., 2013)

3.5 Influence of regional emission and transport

Regional sources and transport can influence the level of air pollution in the Kathmandu Valley mainly originating from regions west of the Kathmandu Valley (Putero et al., 2015). Wind from the north, which is less frequent than southerly and westerly winds, often brings cleaner air mass (also low in CH_4, Figure 4) and hence helps dilute or flush out the valley's polluted air. Household combustion of biofuel, used mainly in the southern plains of Nepal and the IGP region, is an important contributor to the regional pollution in the higher mountainous areas (Panday and Prinn, 2009; Putero et al., 2014). Recently, Putero et al. (2015) attributed the afternoon high BC and O_3 concentrations at Paknajol in the Kathmandu Valley during pre-monsoon season to regional vegetation fire episodes and linked to the regional transport by westerly circulation. Our study also observed a number of episodes with high CO_2, CH_4 and CO

mixing ratios at Bode during most of the days in March, April and May. During the entire sampling period of a year, there were 42 days with CO_2 mixing ratio ≥ 430 ppm, of which 29 days (or 69%) were during the pre-monsoon (25 days or 59% in March and –April alone) and 10 days (23%) in winter. However, atmospheric chemistry transport models are required to confirm and differentiate contributions of local sources and regional sources influencing the Kathmandu Valley, which is beyond the scope of this study.

3.6 CO and CO_2 ratio: Potential emission sources

The ratio of the ambient mixing ratios of CO and CO_2 was used as an indicator to help discriminate emission sources in the Kathmandu Valley. The ratio was calculated from the excess (dCO and dCO_2) relative to the background values of ambient CO and CO_2 mixing ratios. The excess value was estimated by subtracting the base value which was calculated as the fifth percentile of the hourly data for a day (Chandra et al., 2016).

Average emission ratios from the literature are shown in Table 5, and average ratios of dCO/dCO_2 are shown in Table 6, disaggregated into morning hours, evening hours, and seasonal values. Higher ratios were found in pre-monsoon (12.4) and winter (15.1) season compared to post-monsoon (8.3) and monsoon (7.5). These seasonal differences in the dCO/dCO_2 ratio are depicted in Figure 8, which shows a clear relationship with the wind direction and associated emissions, with the highest values especially for stronger westerly winds. Compared to the other three seasons, the ratio in winter was also relatively high for air masses from the east, likely due to emissions from brick kilns combined with accumulation during more stagnant meteorological conditions (supplementary information Figure S2, S3). In other seasons, emission emanating from the north and east of Bode were characterized by a dCO/dCO_2 ratio below 15. Air masses from the west and south generally have a ratio from 20 to 50 in all but post-monsoon season, where the ratio sometimes exceeds 50. A ratio of 50 or over is normally due to very inefficient combustion sources (Westerdahl et al., 2009; Stockwell et al., 2016), such as agro-residue burning, which is common during the post-monsoon season in the Kathmandu Valley.

For interpretability of emission ratio with sources, the ratio was classified into three categories: (i) 0 – 15, (ii) 15 – 45, and (iii) greater than 45. This classification was based on the observed distribution of emission ratio during the study period (Figure 8) and a compilation of observed emission ratios typical for different sources from Nepal and India (see Table 5). An emission ratio below 15 is likely to indicate residential cooking and diesel vehicles, and captive power generation with diesel-powered generator sets (Smith et al., 2000; ARAI, 2008; World Bank, 2014). The emission from brick kilns (FCBTK and Clamp kilns, both common in the Kathmandu Valley), and inefficient, older (built before 2000) gasoline cars fall in between 15 - 45 (Weyant et al., 2014, Stockwell et al., 2016; ARAI, 2008). Four-stroke motorbikes and biomass burning activities (mixed garbage, crop-residue and biomass) are one of the least efficient combustion sources, with emission ratios higher than 45 (Westerdahl et al., 2009; Stockwell et al., 2016; ARAI, 2008).

Based on the classification and Figure 8, the emissions from sources to the north and east of the site are dominated by residential cooking and/or diesel combustion. Emissions from the south and west of Bode are mainly contributed by sources such as brick kilns and inefficient gasoline vehicles. Very high ratios, indicative of agro-residue open burning, generally only show up during the post-monsoon period, when such activities take place, especially in areas southwest of the site. The relatively enhanced ratio (20-30) observed in winds from north and east of the site during winter is mostly likely due to brick kilns that use mixed coal-biomass fuel, whereas the Figure 8 indicates the dominant signature of residential cooking, diesel and old gasoline cars during the pre-monsoon, monsoon and post-monsoon seasons.

The dCO/dCO_2 ratio also changes markedly between the morning peak hours (7:00-9:00, except in winter season when the peak occurs during 8:00-9:00) and evening peak hours (19:00-21:00 pm) (Table 6). Morning and evening values were lowest (2.2, 8.0) during the monsoon and highest (11.2, 21.6) in the winter season, which points to the different emission characteristics in these two seasons. This feature is similar to Ahmedabad, India, another urban site in south Asia, where the morning/evening values were lowest (0.9/19.5) in monsoon and highest in winter (14.3/47.2) (Chandra et al., 2016). In the morning period, the ratio generally falls within a narrower range, from less than 1 to about 25, which indicates a few dominant sources, such as

650 cooking, diesel vehicles, and diesel gen-sets (see Figure 9). In the evening period, the range of
651 the ratio is much wider, from less than 1 to more than 100, especially in winter. This is partly due
652 to the shallower boundary layer in winter, giving local CO emissions a chance to build up more
653 rapidly compared to the longer-lived and well-mixed CO_2, and also indicating the prevalence of
654 additional sources such as brick kilns and agro-residue burning.

655 **3.7 Comparison of CH_4 and CO_2 at semi-urban site (Bode) and rural site (Chanban)**

656 Figure 10 shows time series of hourly average mixing ratios of CH_4, CO_2, CO and water vapor
657 observed simultaneously at Bode and Chanban for the period of 15th July to 3rd October 2015.
658 The hourly meteorological parameters observed at Chanban are shown in supplementary Figure
659 S4. The hourly temperature ranges from 14 to 28.5 °C during the observation period. The site
660 experienced calm winds during the night and moderate southeasterly winds with hourly
661 maximum speed of up to 7.5 m s^{-1} during the observation period. The CH_4 mixing ratios at
662 Chanban varied from 1.880 ppm to 2.384 ppm, and generally increased from the last week of
663 July until early September, peaking around 11th September and then falling off towards the end
664 of the month. CO followed a generally similar pattern, with daily average values ranging from
665 0.10 ppm to 0.28 ppm. The hourly CO_2 mixing ratios ranged from 375 to 453 ppm, with day to
666 day variations, but there were no clear pattern as observed in trend like CH_4 and CO mixing
667 ratios.

668 The CH_4, CO_2, and CO mixing ratios were higher in Bode than in Chanban (Figure 10, Table 4),
669 with Chanban approximately representing the baseline of the lower envelope of the Bode levels.
670 The mean CO_2, CH_4 and CO mixing ratios over the entire sampling period of nearly three
671 months at Bode are 3.8%, 12.1%, and 64% higher, respectively, than at Chanban. The difference
672 in the CO_2 mixing ratio could be due to the large uptake of CO_2 in the forested area at Chanban
673 and surrounding regions compared to Bode, where the local anthropogenic emissions rate is
674 higher and less vegetation for photosynthesis. The coincidence between the base values of CO
675 and CH_4 mixing ratios at Bode and the levels observed at Chanban implies that Chanban CO and
676 CH_4 mixing ratios are indicative of the regional background levels. A similar increase in CO and
677 CH_4 mixing ratios at Chanban from July to September was also observed at Bode, which may

imply that the regional/background levels in the broader Himalayan foothill region also influences the baseline of the daily variability of the pollutants in the Kathmandu Valley, consistent with Panday and Prinn (2009).

Figure 11 shows the comparison of average diurnal cycles of CO_2, CH_4, CO and water vapor mixing ratios observed at Bode and Chanban. The diurnal pattern of CO_2 mixing ratios at both sites is similar, but more pronounced at Bode, with a morning peak around 6:00-7:00, a daytime minimum, and a gradual increase in the evening until the next morning peak. A prominent morning peak at Bode during the monsoon season indicates the influence of local emission sources. The daytime CO_2 mixing ratios are also higher at Bode than at Chanban because of local emissions less uptake of CO_2 for photosynthesis in the valley in comparison to the forested area around Chanban. Like the diurnal pattern of CO_2 depends on the evolution of the mixing layer at Bode, as discussed earlier, it is expected that the mixing layer evolution similarly influences the diurnal CO_2 mixing ratios at Chanban. CO, on the other hand, shows very different diurnal patterns at Bode and Chanban. Sharp morning and evening peaks of CO are seen at Bode, indicating the strong local polluting sources, especially cooking and traffic in the morning and evening peak hours. Chanban, in contrast, only has a subtle morning peak and no evening peak. After the morning peak, CO sharply decreases at Bode but not at Chanban. The growth of the boundary layer after sunrise and entrainment of air from the free troposphere, with lower CO mixing ratios, causes CO to decrease sharply during the day at Bode. At Chanban, on the other hand, since the mixing ratios are already more representative of the local and regional background levels which will also be prevalent in the lower free troposphere, CO does not decrease notably during the daytime growth of the boundary layer as observed at Bode.

Similarly, while there is very little diurnal variation in the CH_4 mixing ratios at Chanban, there is a strong diurnal cycle of CH_4 at Bode, similar to CO_2 there. At Chanban, the CH_4 mixing ratio only shows a weak minimum at around 11 am, a slow increase during the day until a its peak around 22:00, followed by a slow decrease during the night and a more rapid decrease through the morning. The cause of this diurnal pattern at Chanban is presently unclear, but it is clear that the levels are generally representative of the regional background throughout the day and show only limited influences of local emissions.

Atmos. Chem. Phys. Discuss., doi:10.5194/acp-2016-1136, 2017
Manuscript under review for journal Atmos. Chem. Phys.
Discussion started: 2 March 2017

4. **Conclusions**

A cavity ring down spectrometer (Picarro G2401, USA) was used to measure ambient CO_2, CH_4, CO, and water vapor mixing ratios at a semi-urban site (Bode) in the Kathmandu Valley for a year. This was the first 12-months of continuous measurements of these four species in the Kathmandu Valley in the foothills of the central Himalaya. Simultaneous measurement was carried out at a rural site (Chanban) for approximately 3 months to evaluate urban-rural differences.

The measurement also provided an opportunity to establish diurnal and seasonal variation of these species in one of the biggest metropolitan cities in the foothills of Himalayas. Annual average of the mixing ratio of CH_4 and CO_2 in Bode revealed that they were higher than the concentrations at the background sites such as the Mauna Loa, USA and Mt. Waliguan, China, as well as higher than urban/semi-urban sites in nearby regions such as Ahmedabad and Shadnagar in India, and Nanjing in China. These comparisons highlight potential sources of CH_4 and CO_2 in the Kathmandu Valley, such as brick kilns in the valley.

Polluted air masses were transported to the site mainly by two major local wind circulation patterns, East-South/North East and West-Southwest throughout the observation period. Strong seasonality was observed with CO compared to CO_2 and CH_4. Winter and pre-monsoon high CO are linked to emission sources active in these seasons only and are from east-southeast and west-southwest. Emission from the east-southeast are most likely related to brick kilns (winter and pre-monsoon), which are in close proximity to Bode. Major city-centers are located in the west-southwest of Bode (vehicular emission) which impact the site all-round the year, although higher during winter season. Winter high was also observed with CO_2 and CH_4, which are mostly local influence of brick kilns, trash burning and emission from city-center. Nighttime and early morning accumulation of pollutants in winter due to a shallow stable mixing height (200 m) also contribute to elevated levels than other seasons. Regional transport into the Kathmandu Valley could be related to CO_2 peak during pre-monsoon. The highest CH_4 during the post-monsoon could be associated with agricultural activity northeast of Bode. Diurnal variation across all seasons indicates the influence of rush-hour emissions related to vehicles and residential

735 emissions. The evolution of the mixing layer height (200-1200 m) was a major factor which
736 controls the morning-evening peak, afternoon low and night-early morning accumulation or
737 decay. Thus the geographical setting of the Kathmandu Valley and its associated meteorology
738 play a key role in the dispersion and ventilation of pollutants in the Kathmandu Valley. The ratio
739 of CO/CO_2 across different season and wind direction showed that emissions from inefficient
740 gasoline vehicles, brick kilns, residential cooking and diesel combustion are likely to impact
741 Bode.

742 The differences in mean values for urban-rural measurements at Bode and Chanban is highest for
743 CO (64 %) compared to CO_2 (3.8%) and CH_4 (12%). Low values of CH_4 and CO_2 mixing ratios
744 at the Chanban site represent a regional background mixing ratios.

745 This study provided valuable information on key greenhouse gases and air pollutants in the
746 Kathmandu Valley and the surrounding regions, useful for evaluation of satellite measurements
747 climate and regional air quality models. The analysis presented in the paper can provide a sound
748 scientific basis for reducing emissions of greenhouse gases and air pollutants in the Kathmandu
749 Valley.

750 **Acknowledgements**

751 The IASS is grateful for its funding from the German Federal Ministry for Education and
752 Research (BMBF) and the Brandenburg Ministry for Science, Research and Culture (MWFK).
753 This study was partially supported by core funds of ICIMOD contributed by the governments of
754 Afghanistan, Australia, Austria, Bangladesh, Bhutan, China, India, Myanmar, Nepal, Norway,
755 Pakistan, Switzerland, and the United Kingdom as well as funds provided to ICIMOD's
756 Atmosphere Initiative by the Governments of Sweden and Norway. We are thankful to
757 Bhogendra Kathayat, Shyam Newar, Dipesh Rupakheti, Ravi Pokharel, and Pratik Singdan for
758 their assistance during the measurement, P.S. Praveen for his support in calibration of Picarro
759 instrument, Pankaj Sadavarte for his help in refining Figure 1, and Liza Manandhar and Rishi
760 KC for the logistical support. The authors also express their appreciation to the Department of
761 Hydrology and Meteorology (DHM), Nepal, and the Nepal Army.

762 **References**

763

764 Aryal, R. K., Lee, B.-K., Karki, R., Gurung, A., Baral, B., and Byeon, S.-H.: Dynamics of PM
765 2.5 concentrations in Kathmandu Valley, Nepal, Journal of hazardous materials, 168, 732-738,
766 2009.

767

768 Automotive Research Association of India (ARAI).: Emission factor development for Indian
769 vehicles (http://www.cpcb.nic.in/Emission_Factors_Vehicles.pdf), 2008.

770

771 Brun, V. (Eds. 1): Fried earth bricks, kilns and workers in Kathmandu Valley. Himal Books,
772 Lazimpat-Kathmandu, Nepal, 2013.

773

774 Chandra, N., Lal, S., Venkataramani, S., Patra, P. K., and Sheel, V.: Temporal variations of
775 atmospheric CO 2 and CO at Ahmedabad in western India, Atmospheric Chemistry and Physics,
776 16, 6153-6173, 2016.

777

778 Chen, H., Karion, A., Rella, C., Winderlich, J., Gerbig, C., Filges, A., Newberger, T., Sweeney,
779 C., and Tans, P.: Accurate measurements of carbon monoxide in humid air using the cavity ring-
780 down spectroscopy (CRDS) technique, Atmospheric Measurement Techniques, 6, 1031-1040,
781 2013.

782

783 Chen, P., Kang, S., Li, C., Rupakheti, M., Yan, F., Li, Q., Ji, Z., Zhang, Q., Luo, W., and
784 Sillanpää, M.: Characteristics and sources of polycyclic aromatic hydrocarbons in atmospheric
785 aerosols in the Kathmandu Valley, Nepal, Science of the Total Environment, 538, 86-92, 2015.

786

787 Chen, Y. H., and Prinn, R. G.: Estimation of atmospheric methane emissions between 1996 and
788 2001 using a three-dimensional global chemical transport model, Journal of Geophysical
789 Research: Atmospheres, 111, 2006.

790

791 Conrad, R.: Soil microorganisms as controllers of atmospheric trace gases (H2, CO, CH4, OCS,
792 N2O, and NO), Microbiological reviews, 60, 609-640, 1996.

793 Crosson, E.: A cavity ring-down analyzer for measuring atmospheric levels of methane, carbon
794 dioxide, and water vapor, Applied Physics B: Lasers and Optics, 92, 403-408, 2008.

795
796 Department of Transport Management (DoTM).: Annual report of Ministry of Labor and
797 transport management, Nepal Government, 2015.

798

799 Dlugokencky, E.J., A.M. Crotwell, P.M. Lang, J.W. Mund, Atmospheric Methane Dry Air Mole
800 Fractions from quasi-continuous measurements at Mauna Loa, Hawaii, 1986-2015, Version:
801 2016-01-20 (ftp://aftp.cmdl.noaa.gov/data/trace_gases/ch4/in-situ/surface/), 2016

802

803 Fowler, A., and Hennessy, K.: Potential impacts of global warming on the frequency and
804 magnitude of heavy precipitation, Natural Hazards, 11, 283-303, 1995.

805

806 Fragkias, M., Lobo, J., Strumsky, D., and Seto, K. C.: Does size matter? Scaling of CO 2
807 emissions and US urban areas, PLoS One, 8, e64727, 2013.

808

809 Ganesan, A., Chatterjee, A., Prinn, R., Harth, C., Salameh, P., Manning, A., Hall, B., Mühle, J.,
810 Meredith, L., and Weiss, R.: The variability of methane, nitrous oxide and sulfur hexafluoride in
811 Northeast India, Atmospheric Chemistry and Physics, 13, 10633-10644, 2013.

812

813 Goroshi, S. K., Singh, R., Panigrahy, S., and Parihar, J.: Analysis of seasonal variability of
814 vegetation and methane concentration over India using SPOT-VEGETATION and ENVISAT-
815 SCIAMACHY data, Journal of the Indian Society of Remote Sensing, 39, 315-321, 2011.

816

817 Huang, X., Wang, T., Talbot, R., Xie, M., Mao, H., Li, S., Zhuang, B., Yang, X., Fu, C., and
818 Zhu, J.: Temporal characteristics of atmospheric CO 2 in urban Nanjing, China, Atmospheric
819 Research, 153, 437-450, 2015.

820

International Centre for Integrated Mountain Development (ICIMOD).: Himalayas – Water for 1.3 Billion People. Lalitpur. ICIMOD, 2009.

IPCC: Climate Change 2013: The Physical Science Basis. Contribution of Working Group I to the Fifth Assessment Report of the Intergovernmental Panel on Climate Change, Cambridge University Press, Cambridge, United Kingdom and New York, NY, USA, 1535 pp., 2013.

Kim, B. M., Park, J.-S., Kim, S.-W., Kim, H., Jeon, H., Cho, C., Kim, J.-H., Hong, S., Rupakheti, M., and Panday, A. K.: Source apportionment of PM 10 mass and particulate carbon in the Kathmandu Valley, Nepal, Atmospheric Environment, 123, 190-199, 2015.

Kitada, T., and Regmi, R. P.: Dynamics of air pollution transport in late wintertime over Kathmandu Valley, Nepal: As revealed with numerical simulation, Journal of Applied Meteorology, 42, 1770-1798, 2003.

Kumar, M. K., and Nagendra, S. S.: Characteristics of ground level CO_2 concentrations over contrasting land uses in a tropical urban environment, Atmospheric Environment, 115, 286-294, 2015.

Marinoni, A., Cristofanelli, P., Laj, P., Duchi, R., Putero, D., Calzolari, F., Landi, T., Vuillermoz, E., Maione, M., and Bonasoni, P.: High black carbon and ozone concentrations during pollution transport in the Himalayas: Five years of continuous observations at NCO-P global GAW station, Journal of Environmental Sciences, 25, 1618-1625, 2013.

Ministry of Environment (MoE).: Status of climate change in Nepal, Kathmandu Nepal. Kathmandu, Ministry of Environment, 2011.

Ministry of Environment and Forest (MoEF).: Indian Network for Climate Change Assessment: India: Greenhouse Gas Emissions 2007, Tech. rep., 2007.

848 Mues, A., Rupakheti, M., Münkel, C., Lauer, A., Bozem, H., Hoor, P., Butler, T., and Lawrence,
849 M.: Investigation of the mixing layer height derived from ceilometer measurements in the
850 Kathmandu Valley and implications for local air quality. Atmos. Chem. Phys. Discuss,
851 doi:10.5194/acp-2016-1002, in review, 2017.
852
853 Nepal Electricity Authority (NEA)
854 (http://www.nea.org.np/images/supportive_docs/Annual%20Report-2014.pdf), 2014
855 Panday, A. K., and Prinn, R. G.: Diurnal cycle of air pollution in the Kathmandu Valley, Nepal:
856 Observations, Journal of Geophysical Research: Atmospheres, 114, 2009.
857
858 Panday, A. K., Prinn, R. G., and Schär, C.: Diurnal cycle of air pollution in the Kathmandu
859 Valley, Nepal: 2. Modeling results, Journal of Geophysical Research: Atmospheres, 114, 2009.
860 Patra, P., Niwa, Y., Schuck, T., Brenninkmeijer, C., Machida, T., Matsueda, H., and Sawa, Y.:
861 Carbon balance of South Asia constrained by passenger aircraft CO 2 measurements,
862 Atmospheric Chemistry and Physics, 11, 4163-4175, 2011.
863
864 Patra, P., Canadell, J., Houghton, R., Piao, S., Oh, N.-H., Ciais, P., Manjunath, K., Chhabra, A.,
865 Wang, T., and Bhattacharya, T.: The carbon budget of South Asia, 2013.
866
867 Picarro.: Picarro G2401 CO2, CH4, CO, Water vapor CRDS analyzer
868 (http://hpst.cz/sites/default/files/attachments/datasheet-g2401-crds-analyzer-co2-co-ch4-h2o-air-
869 oct15-1.pdf), 2015.
870
871 Prasad, P., Rastogi, S., and Singh, R.: Study of satellite retrieved CO 2 and CH 4 concentration
872 over India, Advances in Space Research, 54, 1933-1940, 2014.
873
874 Pudasainee, D., Sapkota, B., Shrestha, M. L., Kaga, A., Kondo, A., and Inoue, Y.: Ground level
875 ozone concentrations and its association with NOx and meteorological parameters in Kathmandu
876 valley, Nepal, Atmospheric Environment, 40, 8081-8087, 2006.

877 Putero, D., Landi, T., Cristofanelli, P., Marinoni, A., Laj, P., Duchi, R., Calzolari, F., Verza, G.,
878 and Bonasoni, P.: Influence of open vegetation fires on black carbon and ozone variability in the
879 southern Himalayas (NCO-P, 5079 m asl), Environmental Pollution, 184, 597-604, 2014.
880
881 Putero, D., Cristofanelli, P., Marinoni, A., Adhikary, B., Duchi, R., Shrestha, S., Verza, G.,
882 Landi, T., Calzolari, F., and Busetto, M.: Seasonal variation of ozone and black carbon observed
883 at Paknajol, an urban site in the Kathmandu Valley, Nepal, Atmospheric Chemistry and Physics,
884 15, 13957-13971, 2015.
885
886 Regmi, R. P., Kitada, T., and Kurata, G.: Numerical simulation of late wintertime local flows in
887 Kathmandu valley, Nepal: Implication for air pollution transport, Journal of Applied
888 Meteorology, 42, 389-403, 2003.
889
890 Rupakheti, M., Panday, A. K., Lawrence, M. G., Kim, S. W., Sinha, V., Kang, S. C., Naja, M.,
891 Park, J. S., Hoor, P., Holben, B., Sharma, R. K., Mues, A., Mahata, K. S., Bhardwaj, P., Sarkar,
892 C., Rupakheti, D., Regmi, R. P., and Gustafsson, Ö.: Air pollution in the Himalayan foothills:
893 overview of the SusKat-ABC international air pollution measurement campaign in Nepal,
894 Atmos. Chem. Phys. Discuss., in preparation, 2017.
895
896 Sahu, L. K., and Lal, S.: Distributions of C 2–C 5 NMHCs and related trace gases at a tropical
897 urban site in India. Atmos. Environ., 40(5), 880-891, 2006.
898
899 Sarangi, T., Naja, M., S.Lal, Venkataramani, S., Bhardwaj, P., Ojha, N., Kumar, R., Chandola,
900 H. C.: First observations of light non-methane hydrocarbons (C2–C5) over a high altitude site in
901 the central Himalayas, Atmos. Environ., 125, 450–460, 2016.
902
903 Sarangi T., Naja, M., Ojha, N., Kumar, R., Lal, S., Venkataramani, S., Kumar, A., Sagar, R., and
904 Chandola, H. C.: First simultaneous measurements of ozone, CO and NOy at a high altitude
905 regional representative site in the central Himalayas, J. Geophys. Res., 119,
906 doi:10.1002/2013JD020631, 2014.

907

908 Sarkar, C., Sinha, V., Kumar, V., Rupakheti, M., Panday, A., Mahata, K. S., Rupakheti, D.,
909 Kathayat, B., and Lawrence, M. G.: Overview of VOC emissions and chemistry from PTR-TOF-
910 MS measurements during the SusKat-ABC campaign: high acetaldehyde, isoprene and isocyanic
911 acid in wintertime air of the Kathmandu Valley, Atmos Chem Phys, 16, 3979-4003, 2016.
912
913 Schneising, O., Buchwitz, M., Burrows, J., Bovensmann, H., Bergamaschi, P., and Peters, W.:
914 Three years of greenhouse gas column-averaged dry air mole fractions retrieved from satellite–
915 Part 2: Methane, Atmos. Chem. Phys, 9, 443-465, 2009.
916
917 Sharma, R., Bhattarai, B., Sapkota, B., Gewali, M., and Kjeldstad, B.: Black carbon aerosols
918 variation in Kathmandu valley, Nepal, Atmospheric environment, 63, 282-288, 2012.
919
920 Shrestha, R. M., and Rajbhandari, S.: Energy and environmental implications of carbon emission
921 reduction targets: Case of Kathmandu Valley, Nepal, Energy Policy, 38, 4818-4827, 2010.
922
923 Shrestha, S. R., Oanh, N. T. K., Xu, Q., Rupakheti, M., and Lawrence, M. G.: Analysis of the
924 vehicle fleet in the Kathmandu Valley for estimation of environment and climate co-benefits of
925 technology intrusions, Atmospheric Environment, 81, 579-590, 2013.
926
927 Smith, K. R., Uma, R., Kishore, V., Zhang, J., Joshi, V., and Khalil, M.: Greenhouse
928 implications of household stoves: an analysis for India, Annual Review of Energy and the
929 Environment, 25, 741-763, 2000.
930
931 Sreenivas, G., Mahesh, P., Subin, J., Kanchana, A. L., Rao, P. V. N., and Dadhwal, V. K.:
932 Influence of Meteorology and interrelationship with greenhouse gases (CO_2 and CH_4) at a
933 suburban site of India, Atmospheric Chemistry and Physics, 16, 3953-3967, 2016.
934

935 Stockwell, C. E., Christian, T. J., Goetz, J. D., Jayarathne, T., Bhave, P. V., Praveen, P. S.,
936 Adhikari, S., Maharjan, R., DeCarlo, P. F., and Stone, E. A.: Nepal ambient monitoring and
937 source testing experiment (NAMaSTE): emissions of trace gases and light-absorbing carbon
938 from wood and dung cooking fires, garbage and crop residue burning, brick kilns, and other
939 sources, Atmospheric Chemistry and Physics, 16, 11043-11081, 2016.
940
941 Tans, P.: NOAA/ESRL (www.esrl.noaa.gov/gmd/ccgg/trends/) and Keeling, R., Scripps
942 Institution of, Oceanography (scrippsco2.ucsd.edu/), 2014.

943 Westerdahl, D., Wang, X., Pan, X., and Zhang, K. M.: Characterization of on-road vehicle
944 emission factors and microenvironmental air quality in Beijing, China, Atmospheric
945 Environment, 43, 697-705, 2009.
946
947 Weyant, C., Athalye, V., Ragavan, S., Rajarathnam, U., Lalchandani, D., Maithel, S., Baum, E.,
948 and Bond, T. C.: Emissions from South Asian brick production, Environmental science &
949 technology, 48, 6477-6483, 2014.
950
951 World Bank: Managing Nepal's Urban Transition
952 (http://www.worldbank.org/en/news/feature/2013/04/01/managing-nepals-urban-transition),
953 2013.
954
955 World Bank: Diesel power generation: inventories, black carbon emissions in Kathmandu
956 Valley, Nepal. Washington. The World Bank: 1818H Street NW, Washington, DC 20433, USA

957 WMO: The state of greenhouse gases in the atmosphere based on global observations through
958 2015
959 (http://reliefweb.int/sites/reliefweb.int/files/resources/GHG_Bulletin_12_EN_web_JN161640.pd
960 f), 2016.

961

962

Atmos. Chem. Phys. Discuss., doi:10.5194/acp-2016-1136, 2017
Manuscript under review for journal Atmos. Chem. Phys.
Discussion started: 2 March 2017

Atmospheric Chemistry and Physics Discussions

Table 1. Instruments and sampling at Bode (semi-urban site) and Chanban (rural site)

Site	Instrument	Species	sampling interval	Measurement period	inlet/sensor height above ground (m)
Bode	i. Cavity ring down spectrometer (Picarro G2401, USA)	CO_2, CH_4, CO, water vapor	5 sec	06 Mar 2013 - 05 Mar 2014 14 Jul 2015 - 07 Aug 2015	20
	ii. CO monitor (Horriba AP370, USA)	CO	5 min	06 Mar 2013 – 07 June 2013	20
	iii. Ceilometer (Vaisala CL31, Finland		15-52 min	06 Mar 2013 – 05 Mar 2014	15
	iv. AWS (Campbell Scientific, USA)		1 min		23
	a. CS215	RH, T		06 Mar 2013 – 24 Apr 2013	
	b. CS300 Pyranometer	SR		06 Mar 2013 - 05 Mar 2014 14 Jul 2015 - 07 Aug 2015	
	c. RM Young 05103-5	WD, WS		06 Mar 2013 - 05 Mar 2014 14 July 2015 - 07 Aug 2015	
	v. Airport AWS (Environdata, Australia)				
	a. TA10	T		18 Jun 2013 – 13 Jan 2013	
	b. RG series	RF		06 Mar 2013 – 15 Dec 2013	
Chanban	i. Cavity ring down spectrometer (Picarro G2401, USA)	CO_2, CH_4, CO, water vapor	5 sec	15 July 2015 - 03 Oct 2015	3
	ii AWS (Davis Vantage Pro2, USA)	RH, T, SR, WD, WS, RF, P	10 min	14 July 2015 - 07 Aug 2015	2

AWS: Automatic weather station, RH: ambient relative humidity, T: ambient temperature, SR: global solar radiation, WS: wind speed, WD: wind direction, RF: rainfall, P: ambient pressure

Atmos. Chem. Phys. Discuss., doi:10.5194/acp-2016-1136, 2017
Manuscript under review for journal Atmos. Chem. Phys.
Discussion started: 2 March 2017

Atmospheric Chemistry and Physics Discussions

Table 2. Summary of monthly average CH_4 and CO_2 mixing ratios observed at Bode, a semi-urban site in the Kathmandu Valley during March 2013 to Feb 2014 [mean, standard deviation (SD), median, minimum (Min.), maximum (Max.) and number of data points of hourly average values]

	CH_4 (ppm)					CO_2 (ppm)					
Month	Mean	SD	Median	Min.	Max.	Mean	SD	Median	Min.	Max.	Data points
Mar	2.207	0.245	2.152	1.851	3.094	426.6	26.4	418.3	378.8	510.8	596
Apr	2.183	0.252	2.094	1.848	3.121	430.3	27.4	421.0	397.0	536.9	713
May	2.093	0.174	2.040	1.863	2.788	421.7	22.1	413.4	395.9	511.2	725
Jun	2.061	0.142	2.017	1.869	2.675	417.9	21.3	410.4	390.5	495.7	711
Jul	2.129	0.168	2.074	1.893	2.770	410.3	18.2	406.3	381.0	471.0	500
Aug	2.274	0.260	2.181	1.953	3.219	409.9	22.8	405.3	376.1	493.1	737
Sep	2.301	0.261	2.242	1.941	3.331	414.9	30.2	404.0	375.9	506.2	710
Oct	2.210	0.195	2.156	1.927	2.762	417.0	25.1	411.8	381.9	486.7	743
Nov	2.207	0.203	2.178	1.879	2.705	417.2	20.7	415.7	385.7	478.9	717
Dec	2.206	0.184	2.193	1.891	2.788	417.7	17.3	418.0	386.7	467.6	744
Jan	2.233	0.219	2.198	1.889	2.744	424.8	20.9	422.3	392.7	494.5	696
Feb	2.199	0.223	2.152	1.877	2.895	423.2	22.0	417.9	392.2	484.6	658
Annual	2.193	0.224	2.134	1.848	3.331	419.4	23.9	414.0	375.9	536.9	8353

Atmos. Chem. Phys. Discuss., doi:10.5194/acp-2016-1136, 2017
Manuscript under review for journal Atmos. Chem. Phys.
Discussion started: 2 March 2017

Atmospheric Chemistry and Physics Discussions

Table 3. Summary of CH_4 and CO_2 mixing ratios at Bode across four seasons during March 2013 to Feb 2014 [seasonal mean, one standard deviation (SD), median, minimum (Min.) and maximum (Max.)]

	CH_4 (ppm)					CO_2 (ppm)				
Season	Mean	SD	Median	Min.	Max.	Mean	SD	Median	Min.	Max.
Pre-Monsoon	2.157	0.230	2.082	1.848	3.121	426.2	25.5	417.0	378.8	536.9
Monsoon	2.199	0.241	2.126	1.869	3.331	413.5	24.2	407.1	375.9	506.2
Post-Monsoon	2.210	0.200	2.167	1.879	2.762	417.3	23.1	414.1	381.9	486.7
Winter	2.214	0.209	2.177	1.877	2.895	421.9	20.3	419.3	386.7	494.5

Atmos. Chem. Phys. Discuss., doi:10.5194/acp-2016-1136, 2017
Manuscript under review for journal Atmos. Chem. Phys.
Discussion started: 2 March 2017

Atmospheric Chemistry and Physics Discussions

Table 4. Comparison of monthly average CH_4 and CO_2 mixing ratios at a semi-urban and a rural site in Nepal (this study) with other urban and background sites in the region and elsewhere

Site Setting	Bode, Nepal (Urban)				Chanban, Nepal (Rural)		Mauna Loa, USA (Background)[d]		Waliguan, China (Background)[e]	
Species	CO_2	CH_4	CO_2	CH_4	CO_2	CH_4	CO_2	CH_4	CO_2	CH_4
Unit	ppm	ppb	Ppm	ppb	ppm	ppb	ppm	ppb	ppm	ppb
Mar 2013	426.6	2207.06					397.3	1839.82	399.5	1867.54
Apr	430.3	2183.30					398.4	1836.65	402.8	1874.03
May	421.7	2093.46					399.8	1833.66	402.5	1877.53
Jun	417.9	2060.91					398.6	1817.77	397.4	1887.36
Jul	410.3	2129.54					397.2	1808.36	393.3	1887.63
Aug	409.9	2274.34	411.3	2281.11	403.4	2049.71	395.2	1819.13	392.0	1892.78
Sep	414.9	2301.35	419.9	2370.93	399.1	2101.75	393.5	1835.79	393.1	1893.48
Oct	417.0	2210.02					393.7	1835.90	395.6	1876.36
Nov	417.2	2206.84					395.1	1834.49	397.1	1875.09
Dec	417.7	2205.91					396.8	1844.66	398.6	1880.21
Jan 2014	424.8	2233.82					397.8	1842.20	398.8	1865.45
Feb	423.2	2199.01					397.9	1833.51	401.1	1877.64
Annual										
Bode	419.4	2193.07								
Mauna Loa							396.8	1831.83		
Waliguan									397.7	1879.59
Nanjing (2011)[a]	406.5									
Shadnagar (2014)[b]	394.0									
Ahemadabad (2013-2015)[c]	413.0	1920.0								

[a] Huang et al., 2015, [b] Sreenivas et al., 2016, [c] Chandra et al., 2016, [d] ftp://aftp.cmdl.noaa.gov/data/trace_gases/ch4/in-situ/surface/mlo/; ftp://aftp.cmdl.noaa.gov/data/trace_gases/co2/in-situ/surface/mlo/, [e] ftp://aftp.cmdl.noaa.gov/data/trace_gases/co2/flask/surface/wlg/; ftp://aftp.cmdl.noaa.gov/data/trace_gases/ch4/flask/surface/wlg/

Atmos. Chem. Phys. Discuss., doi:10.5194/acp-2016-1136, 2017
Manuscript under review for journal Atmos. Chem. Phys.
Discussion started: 2 March 2017

Atmospheric Chemistry and Physics Discussions

Table 5. Emission ratio of CO/CO_2 (ppb ppm^{-1}) derived from emission factors (gram of gas emitted from per kilogram of fuel burned, except transport sector which is derived from gram of gases emitted per kilometer distance travelled)

Sectors	Details	CO/CO_2	Reference
1. Residential/Commercial			
i. LPG		4.8	Smith et al. (2000)
ii. Kerosene		13.4	Smith et al. (2000)
iii. Biomass		52.9 - 98.5	*
iv. Diesel power generators	< 15 year old	5.8	The World Bank (2014)
	>15 year old	4.5	
2. Transport			**
a. Diesel			
i. HCV diesel bus	>6000cc, 1996-2000	4.9	
	post 2000 and 2005	5.4	
ii. HCV diesel truck	>6000cc, post 2000	7.9	
b. Petrol			
i. 4 stroke motorcycle	<100 cc, 1996-2000	68	
	100-200 cc, Post 2000	59.6	
ii. Passenger cars	<1000 cc, 1996-2000	42.4	
iii. Passenger cars	<1000 cc, Post 2000	10.3	
3. Brick industries			
i. BTK fixed kiln		17.2	Weyant et al. (2014)
ii. Clamp brick kiln		33.7	Stockwell et al. (2016)
iii. Zigzag brick kiln		3.9	Stockwell et al. (2016)
4. Open burning			
i. Mixed garbage		46.9	Stockwell et al. (2016)
ii. Crop-residue		51.6	Stockwell et al. (2016)

* Westerdahl et al. (2009)
** http://www.cpcb.nic.in/Emission_Factors_Vehicles.pdf

Atmos. Chem. Phys. Discuss., doi:10.5194/acp-2016-1136, 2017
Manuscript under review for journal Atmos. Chem. Phys.
Discussion started: 2 March 2017

Atmospheric Chemistry and Physics Discussions

Table 6. Seasonal average of the ratio of dCO to dCO_2 over a period of 3 hours during (a) morning peak and (b) evening peak in the ambient mixing ratios of CO and CO_2

Period	Season	dCO/dCO_2 (SD)	Median	N	Confidence interval (95%)
a. Morning hours (7:00-9:00)	Pre-monsoon	7.6 (3.1)	7.8	249	0.4
	Monsoon	2.2 (1.6)	1.9	324	0.2
	Post-monsoon	3.1 (1.4)	2.8	183	0.2
	Winter*	11.2 (4.4)	11.0	255	0.5
b. Evening hours (19:00-21:00)	Pre-monsoon	15.1 (9.0)	12.7	248	1.1
	Monsoon	8.0 (5.2)	6.3	323	0.6
	Post-monsoon	11.5 (5.6)	10.6	182	0.8
	Winter	21.6 (14.1)	18.2	254	1.7
c. Seasonal (all hours)	Pre-monsoon	12.2 (13.3)	8.8	1740	0.6
	Monsoon	7.5 (13.5)	2.9	2176	0.6
	Post-monsoon	8.3 (12.4)	4.4	1289	0.7
	Winter	15.1 (13.3)	12.5	1932	0.6

Atmos. Chem. Phys. Discuss., doi:10.5194/acp-2016-1136, 2017
Manuscript under review for journal Atmos. Chem. Phys.
Discussion started: 2 March 2017

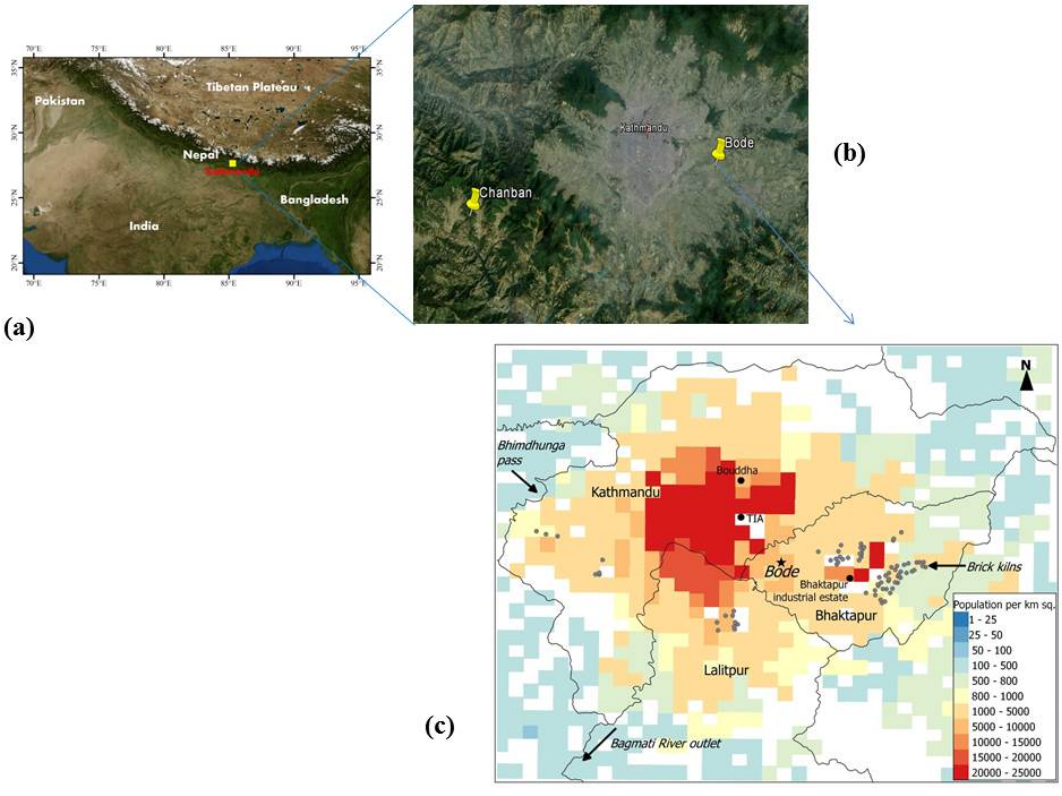

Figure 1. Location of measurement sites: (a) Kathmandu Valley (b) semi-urban measurement site at Bode in Kathmandu Valley, and a rural measurement site at Chanban in Makawanpur district Nepal, (c) general setting of Bode site. Colored grid and TIA represent population density and the Tribhuvan International Airport, respectively.

Atmos. Chem. Phys. Discuss., doi:10.5194/acp-2016-1136, 2017
Manuscript under review for journal Atmos. Chem. Phys.
Discussion started: 2 March 2017

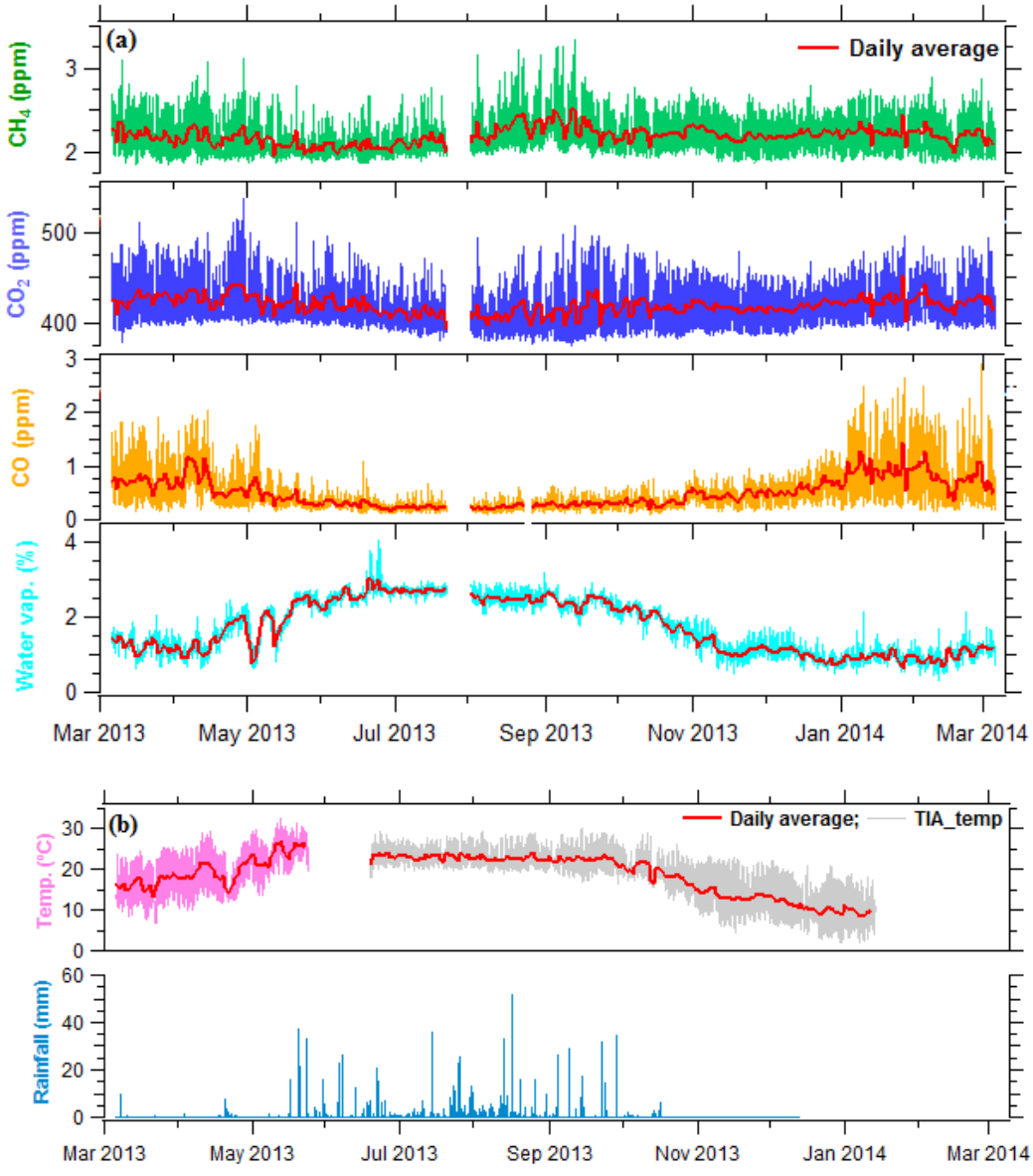

Figure 2. Time series of hourly average (a) mixing ratios of CH_4, CO_2, CO, and water vapor measured with a cavity ring down spectrometer (Picarro G2401) at Bode, and (b) temperature and rainfall monitored at the Tribhuvan International Airport (TIA), ~4 km to the west of Bode site in the Kathmandu Valley, Nepal. Temperature shown in pink color is observed at Bode site.

Atmos. Chem. Phys. Discuss., doi:10.5194/acp-2016-1136, 2017
Manuscript under review for journal Atmos. Chem. Phys.
Discussion started: 2 March 2017

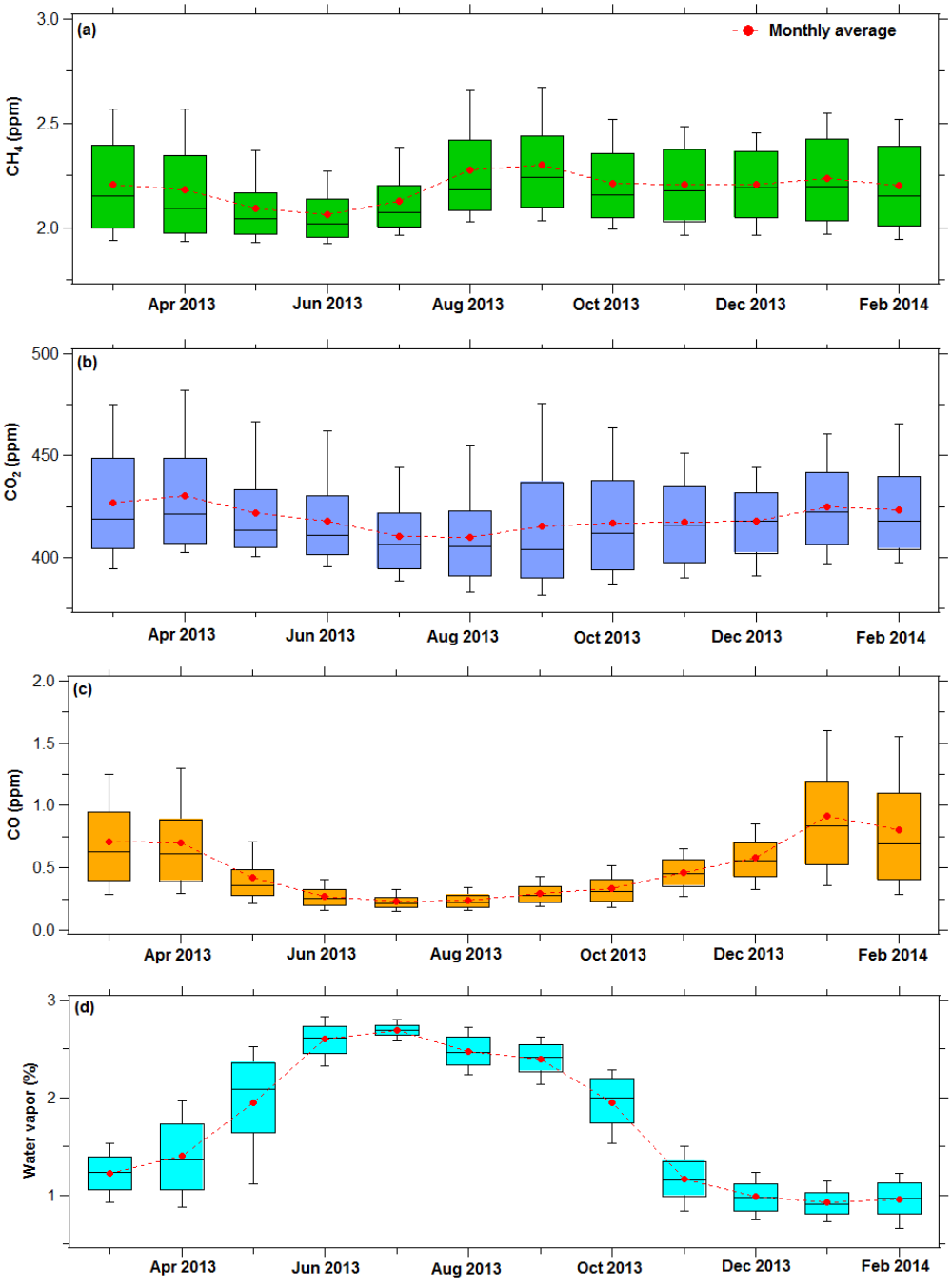

Atmos. Chem. Phys. Discuss., doi:10.5194/acp-2016-1136, 2017
Manuscript under review for journal Atmos. Chem. Phys.
Discussion started: 2 March 2017

Atmospheric Chemistry and Physics Discussions

Figure 3. Monthly variations of the mixing ratios of hourly (a) CH_4, (b) CO_2, (c) CO, and (d) water vapor observed at a semi-urban site (Bode) in the Kathmandu Valley over a period of a year. The lower end and upper end of the whisker represents 10^{th} and 90^{th} percentile, respectively; the lower end and upper end of each box represents 25^{th} and 75^{th} percentile, respectively, and black horizontal line in the middle of each box is the median for each month while red dot represents mean for each month.

Atmos. Chem. Phys. Discuss., doi:10.5194/acp-2016-1136, 2017
Manuscript under review for journal Atmos. Chem. Phys.
Discussion started: 2 March 2017

Atmospheric Chemistry and Physics Discussions

(a)

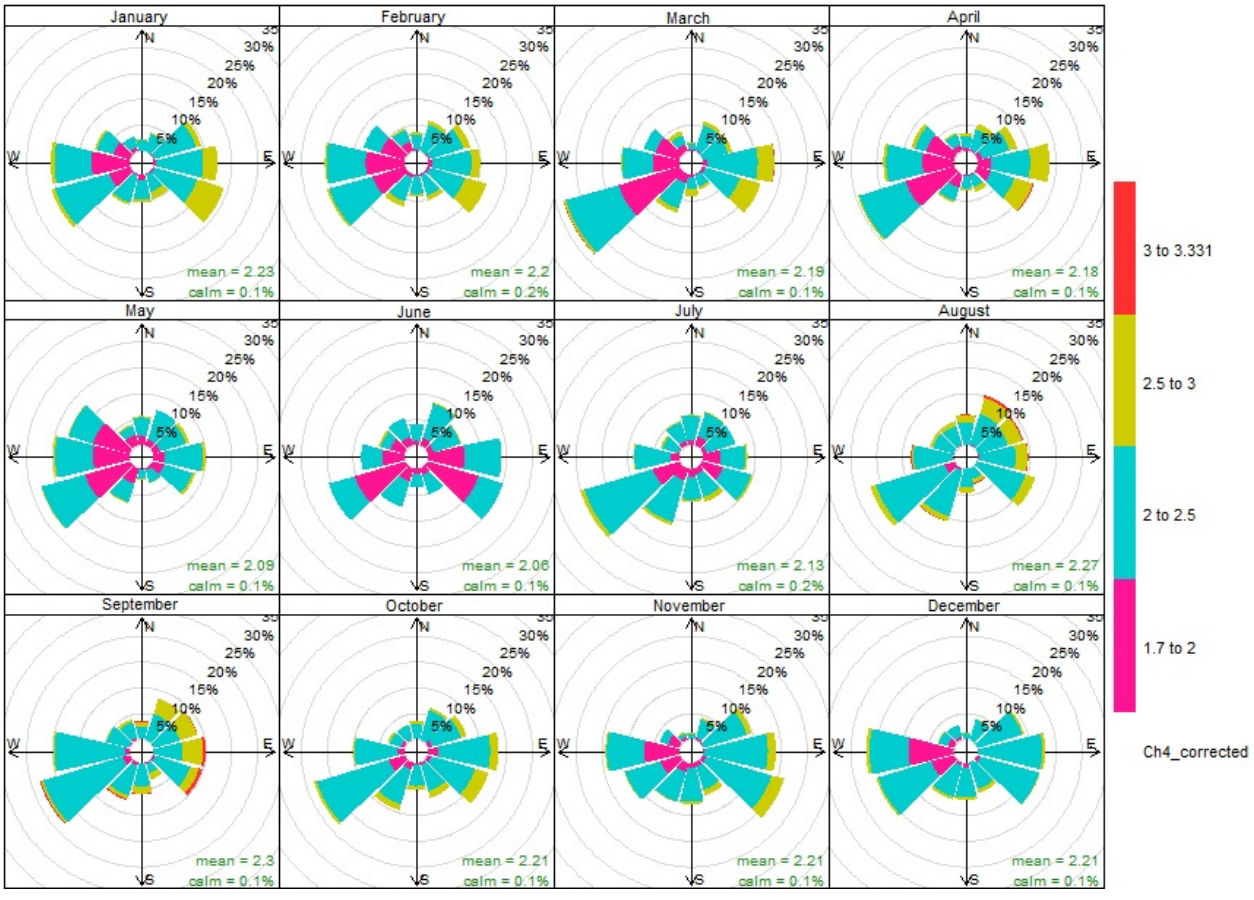

Atmos. Chem. Phys. Discuss., doi:10.5194/acp-2016-1136, 2017
Manuscript under review for journal Atmos. Chem. Phys.
Discussion started: 2 March 2017

Atmospheric Chemistry and Physics Discussions

(b)

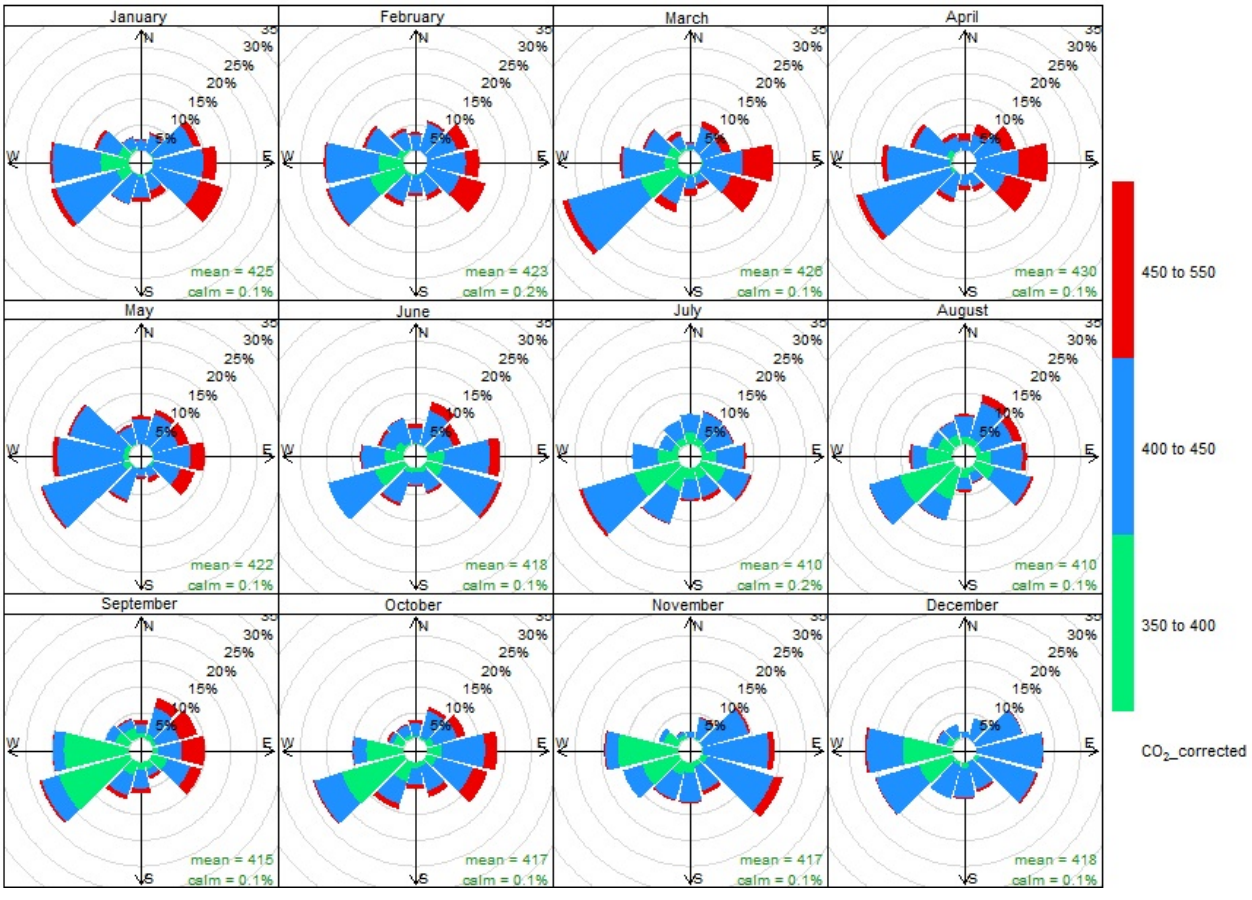

Atmos. Chem. Phys. Discuss., doi:10.5194/acp-2016-1136, 2017
Manuscript under review for journal Atmos. Chem. Phys.
Discussion started: 2 March 2017

Atmospheric Chemistry and Physics Discussions

Figure 4. Pollution rose of the hourly CH_4 and CO_2 mixing ratios observed at Bode in the Kathmandu Valley (a) CH_4 and (b) CO_2 from Mar 2013 to Feb 2014. Pollution rose shows variations of pollutants based on frequency of counts by wind direction. The units of CH_4 and CO_2 are in ppm

Atmos. Chem. Phys. Discuss., doi:10.5194/acp-2016-1136, 2017
Manuscript under review for journal Atmos. Chem. Phys.
Discussion started: 2 March 2017

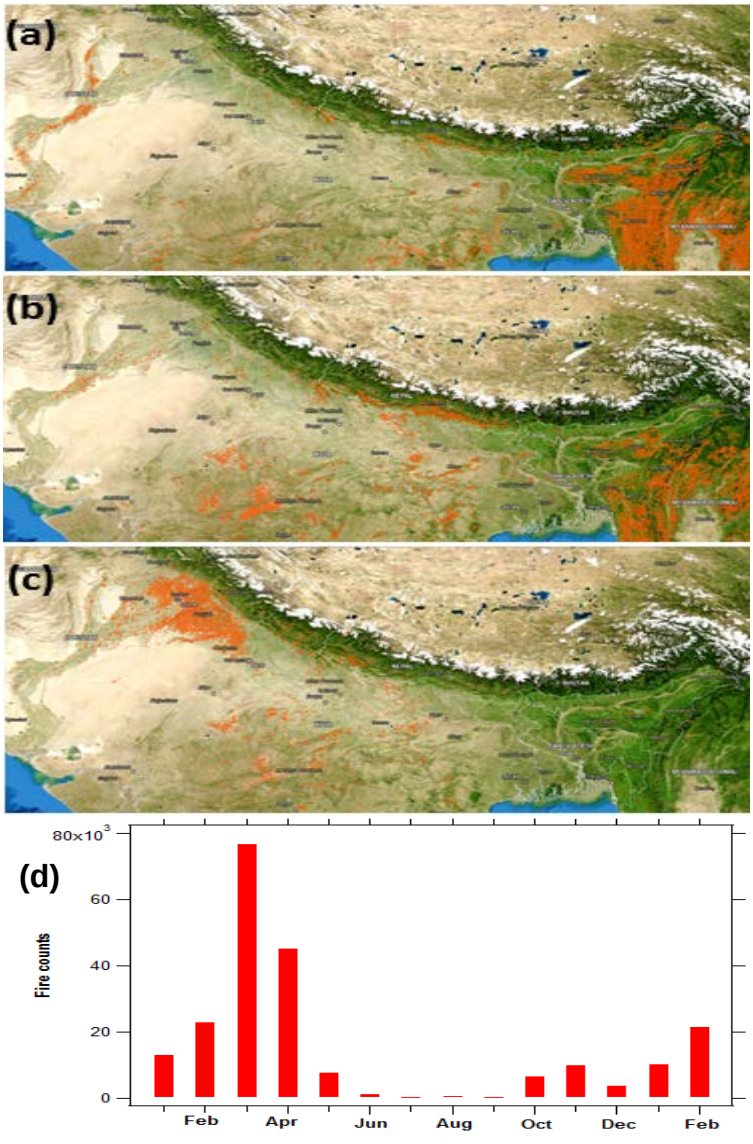

Figure 5. Satellite detected fire counts in (a) Mar, (b) Apr, (c) May 2013 in the broader region surrounding Nepal and (d) total number of fire counts detected by MODIS instrument onboard the Aqua satellite during Jan 2013-Feb 2014. Source: https://firms.modaps.eosdis.nasa.gov/firemap/

Atmos. Chem. Phys. Discuss., doi:10.5194/acp-2016-1136, 2017
Manuscript under review for journal Atmos. Chem. Phys.
Discussion started: 2 March 2017

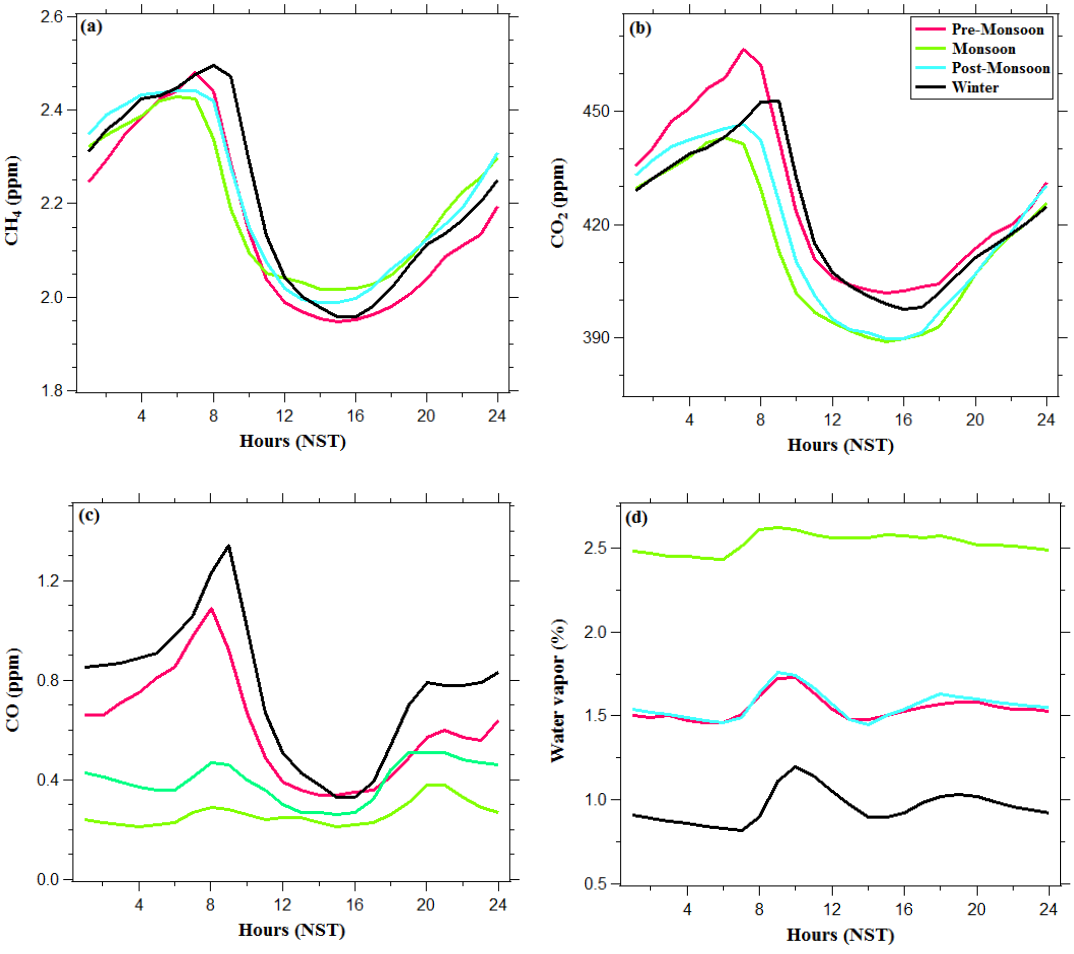

Figure 6. Diurnal variations of hourly mixing ratios in different seasons (a) CH_4, (b) CO_2, (c) CO, and (d) water vapor observed at Bode (semi-urban site) in the Kathmandu Valley during March 2013-February 2014. Seasons are defined as Pre-monsoon: Mar-May, Monsoon: Jun-Sep, Post-monsoon: Oct-Nov, Winter: Dec-Feb. The x axis is in Nepal Standard Time (NST).

Atmos. Chem. Phys. Discuss., doi:10.5194/acp-2016-1136, 2017
Manuscript under review for journal Atmos. Chem. Phys.
Discussion started: 2 March 2017

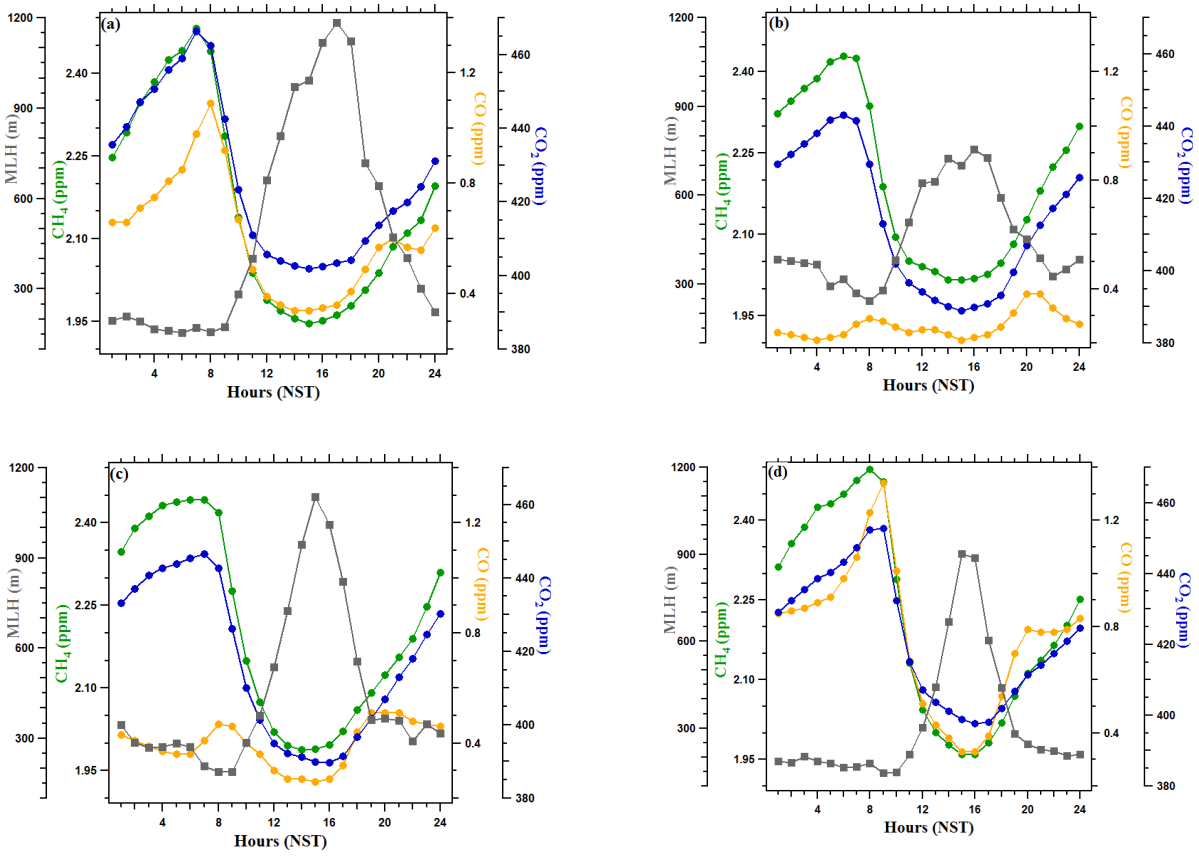

Atmos. Chem. Phys. Discuss., doi:10.5194/acp-2016-1136, 2017
Manuscript under review for journal Atmos. Chem. Phys.
Discussion started: 2 March 2017

Atmospheric Chemistry and Physics Discussions

Figure 7. Diurnal variations of hourly mixing ratios of CH_4, CO_2, CO, and mixing layer height (MLH) at Bode (a semi-urban site in the Kathmandu Valley) in different seasons (a) pre-monsoon (Mar-May), (b) monsoon (Jun-Sep), (c) post-monsoon (Oct-Nov) and (d) winter (Dec-Feb) during March 2013- Feb 2014.

Atmos. Chem. Phys. Discuss., doi:10.5194/acp-2016-1136, 2017
Manuscript under review for journal Atmos. Chem. Phys.
Discussion started: 2 March 2017

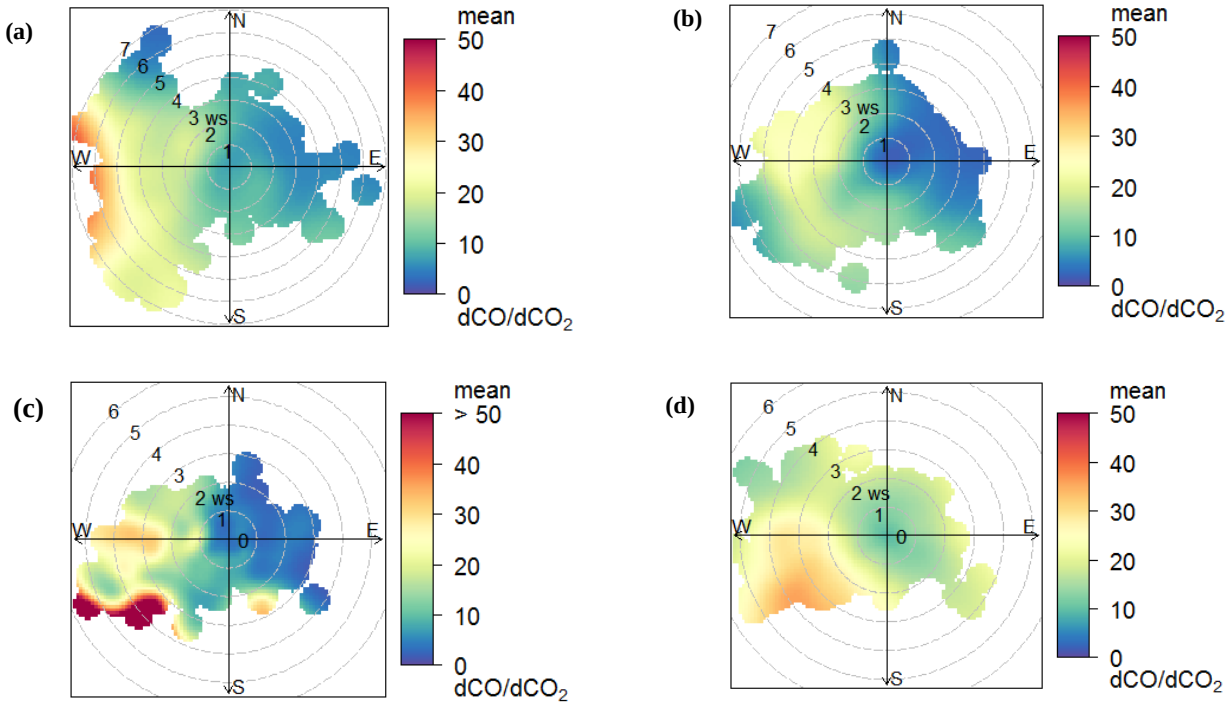

Figure 8. Seasonal polar plot of hourly dCO/dCO_2 ratio based upon wind direction and wind speed: (a) pre-monsoon, (b) monsoon, (c) post-monsoon and (d) winter seasons.

Atmos. Chem. Phys. Discuss., doi:10.5194/acp-2016-1136, 2017
Manuscript under review for journal Atmos. Chem. Phys.
Discussion started: 2 March 2017

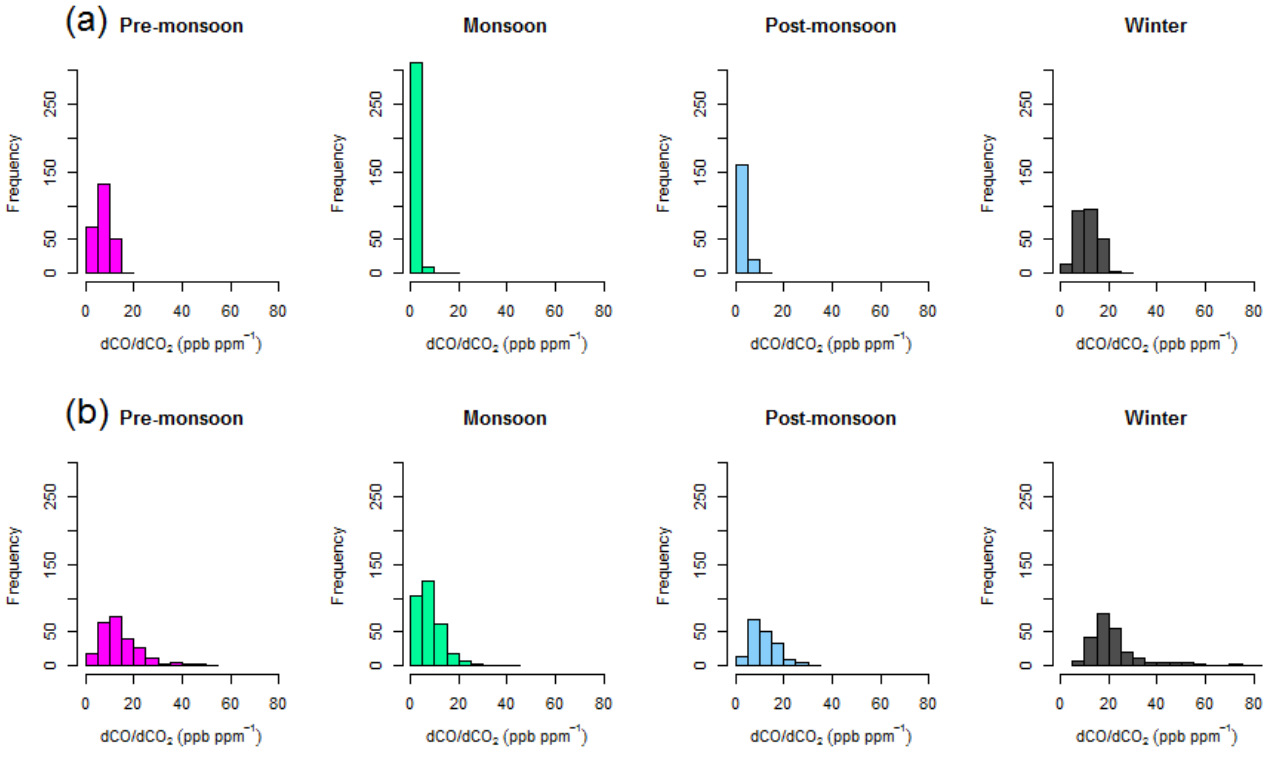

Figure 9. Seasonal frequency distribution of hourly dCO/dCO_2 ratio (a) morning hours (7:00-9:00) in all season except winter (8:00-10:00), (b) evening hours (19:00-21:00)

Atmos. Chem. Phys. Discuss., doi:10.5194/acp-2016-1136, 2017
Manuscript under review for journal Atmos. Chem. Phys.
Discussion started: 2 March 2017

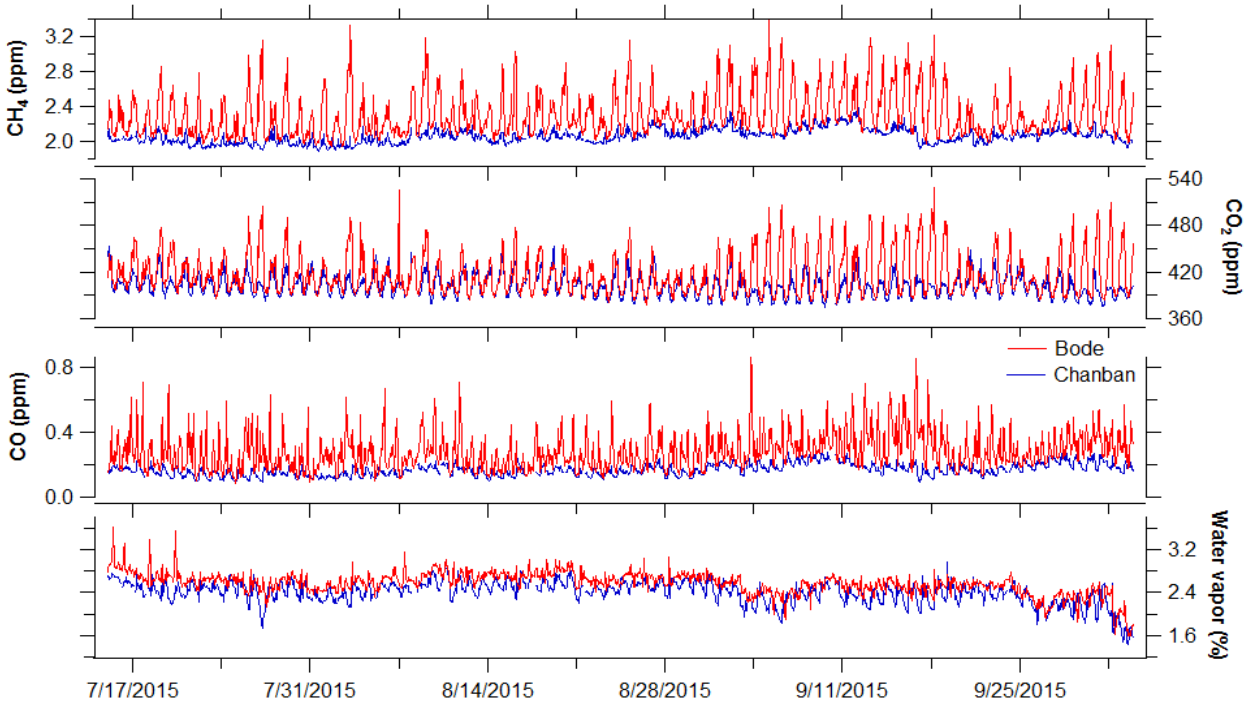

Figure 10. Comparison of hourly average mixing rations of CH_4, CO_2, CO, and water vapor observed at Bode (a semi-urban site) in the Kathmandu Valley and at Chanban (a rural/background site) in Makawanpur district, ~ 20 km from Kathmandu, on other side of a tall ridge.

Atmos. Chem. Phys. Discuss., doi:10.5194/acp-2016-1136, 2017
Manuscript under review for journal Atmos. Chem. Phys.
Discussion started: 2 March 2017

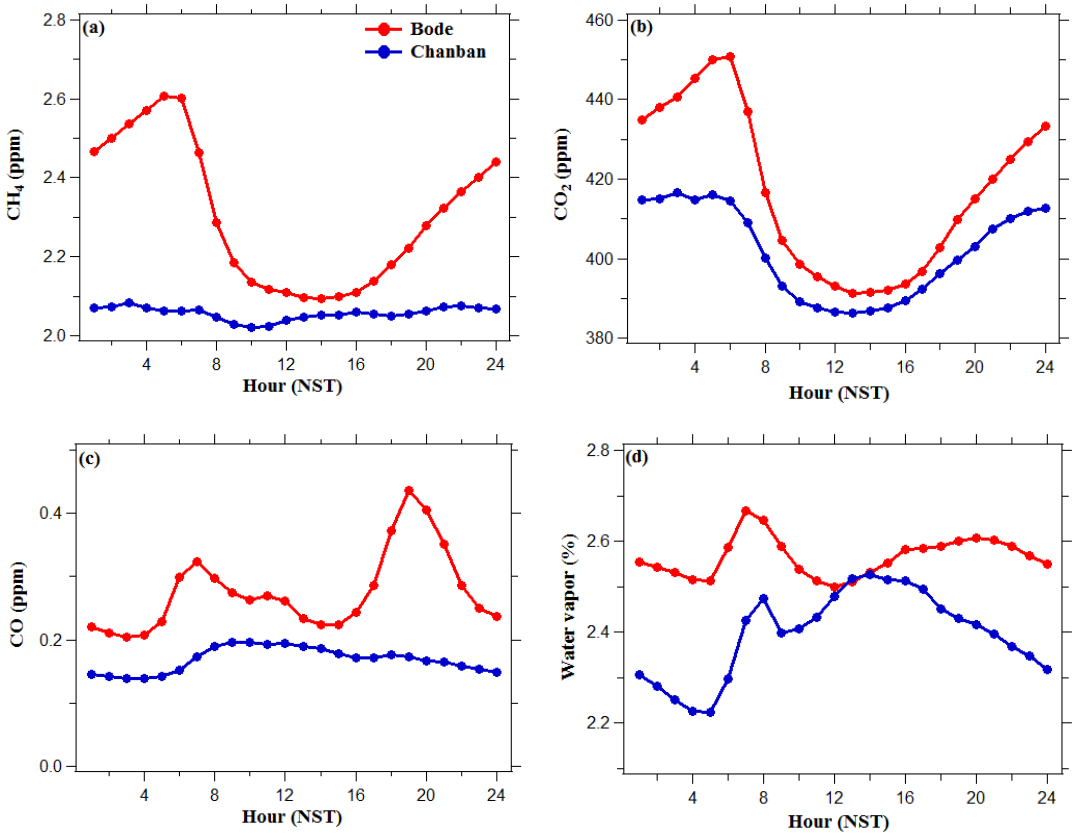

Figure 11. Diurnal variations of hourly average mixing ratios of (a) CH_4, (b) CO_2, (c) CO and (d) water vapor observed at Bode in the Kathmandu Valley and at Chanban in Makawanpur district during 15 July- 03 October 2015